From the DEPARTMENT OF PHYSIOLOGY AND PHARMACOLOGY
Karolinska Institutet, Stockholm, Sweden

OXIDATIVE STRESS AND MUSCLE WEAKNESS ASSOCIATED WITH RHEUMATOID ARTHRITIS

Maarten Michiel Steinz

Karolinska Institutet

Stockholm 2020

Published by Karolinska Institutet.
Printed by Universitetsservice US-AB 2020

ISBN 978-91-7831-716-5

Oxidative stress and muscle weakness associated with rheumatoid arthritis

THESIS FOR DOCTORAL DEGREE (Ph.D.)

By

Maarten Michiel Steinz

Principal Supervisor:
Ass. Prof. Dr. Johanna Lanner
Karolinska Institutet
Department of Physiology & Pharmacology
Division of Molecular Muscle Physiology & Pathophysiology

Co-supervisors:
Prof. Dr. Camilla Svensson
Karolinska Institutet
Department of Physiology & Pharmacology
Division of Molecular Pain Research

Prof. Dr. Thomas Gustafsson
Karolinska Institutet
Department of Laboratory Medicine
Division of Clinical Physiology

Opponent:
Prof. Dr. Malcolm Jackson
University of Liverpool
Department of Musculoskeletal Biology

Examination Board:
Prof. Dr. Fredrik Elinder
Linköping University
Department of Clinical and Experimental Medicine

Prof. Dr. Anna Krook
Karolinska Institutet
Department of Physiology and Pharmacology

Prof. Dr. Bent Winding Deleuran
Aarhus University
Department of Biomedicine

Public defense February 21, 2020, 9:00

Karolinska Institutet Biomedicum 1

Solnavägen 9, 17165, Stockholm, Sweden

To my parents

POPULAR SCIENTIFIC SUMMARY

From walking the dog to playing a sport: in our everyday life we use muscles to perform almost any task. Therefore, muscle weakness can severely reduce the quality of life. That is what happens in patients with a chronic inflammatory disease, such as rheumatoid arthritis. Up until today it is however not well understood how a chronic inflammation causes muscle weakness.

Rheumatoid arthritis is one of the world's most prevalent chronic inflammatory diseases. It affects women more often than men. Patients with rheumatoid arthritis, have an inflammation in their joints. Skeletal muscles are attached via the tendons to the joints which makes it possible to perform many different types of movements. An inflammation in the joint can therefore have severe effects on the muscles that surround it. In fact, scientific research has previously shown that the joint inflammation in rheumatoid arthritis causes the muscles to become weak. Muscle weakness in rheumatoid arthritis has been associated with a decrease in muscle mass. However, a decrease in muscle mass cannot solely explain why rheumatoid arthritis patients have weaker muscles than healthy persons. We measured the muscle strength of the legs of rheumatoid arthritis patients and of mice with arthritis and we, interestingly, saw that the muscle strength was decreased while the muscles were not smaller compared to healthy subjects. The weakness in the RA patients could neither be explained by a decrease in their daily activity, because we measured that the healthy individuals and RA patients were equally active. To understand what is happening instead, we took a closer look inside the muscle.

Muscles contain many proteins, when these proteins get damaged, their normal functioning may change. The damage on muscle proteins can be oxidative damage which is caused by reactive molecules that can attack the building stones of the proteins, i.e. the amino acids. The reactive molecules that cause oxidative damage are called reactive oxygen species. They are produced under normal circumstances at many places in our body, also inside the muscles, and are continuously cleared away by the body's own antioxidant system. However, when the production of reactive oxygen species exceeds their clearance, they can cause damage on protein amino acids which is called oxidative stress. Interestingly, previous research has shown that rheumatoid arthritis patients have more oxidative stress in their muscles which has been associated with muscle weakness. Up until today it was however not clear how that happens.

Some of the most important proteins that regulate muscle strength are both the ryanodine receptor and actin. The ryanodine receptor is located at the storage place for calcium ions, the so-called sarcoplasmic reticulum. Calcium ions enable the muscles to produce force and the release of calcium from the sarcoplasmic reticulum is tightly controlled by the gatekeeper: the ryanodine receptor. We showed that the ryanodine receptor loses its tight control of calcium release when it gets damaged by oxidative stress: it increases its probability to be open, whereby calcium can flow through the channel. An increased open probability of the ryanodine receptor is associated with calcium leak from the sarcoplasmic reticulum which

can thereby lead to decreased calcium storage and decreased muscle force production. In addition to the ryanodine receptor we also looked at the effects of oxidative stress on actin. Actin is one of the main components of the smallest muscle units that researchers can measure force on: the myofibrils. Our measurements showed that when myofibrils are damaged by oxidative stress, the force of the myofibrils decreases. To further understand the force producing machinery, we took a closer look at actin itself. Many actin proteins together form a long filament of actin, which is the centrally located filament of a myofibril. When we introduced oxidative damage on actin its ability to form a long actin filament was impaired.

To further understand how oxidative stress can cause all these detrimental effects, we identified which exact amino acids (i.e. the protein building stones) of the ryanodine receptor and actin that get damaged by oxidative stress. We showed that the damage was introduced at specific amino acids that are located in important positions of the structure of ryanodine and actin. The damaged amino acids in these locations can indeed impair their normal function: i.e. increase the probability of that the ryanodine receptor is in an open state, decrease myofibrillar force and decrease the stability of actin. So the important question we then asked ourselves: could we identify the exact same damaged amino acids also in the ryanodine receptor and actin of the weaker muscles from rheumatoid arthritis patients and mice with arthritis? Intriguingly, yes indeed: in actin from weakened muscle of mice with arthritis and patients with RA we found exactly the same modified amino acids of which we have shown that they can cause decreased myofibrillar force and decreased actin stability. Taken together, we could therefore conclude that oxidative stress on actin contributes to muscle weakness in association with rheumatoid arthritis.

Since the patients of our study were on conventional anti-rheumatic medication but still exhibited muscle weakness, the previously described results stress the need of additional medications that can counteract muscle weakness induced by oxidative stress in rheumatoid arthritis patients. There are however three important things to consider when we want to counteract oxidative stress in weakened muscles afflicted with RA. Firstly, and as mentioned before, reactive oxygen species are produced at many places in our body and our muscles, also under normal circumstances. Secondly, reactive oxygen species immediately react with everything that is near, thus most likely immediately at the places of their production. At last, it is important to know that our body can produce its own antioxidants that can clear reactive oxygen species that are produced too much and at the wrong place (e.g. near muscle proteins that regulate muscle force such as actin). We therefore aimed to find out which specific reactive oxygen species were responsible for the oxidative damage in muscles afflicted with arthritis. In addition, we also looked at the location of the body's own antioxidants in arthritis-afflicted muscles.

The main sources of the reactive oxygen species in muscles are considered to be the mitochondria and NOX2. Through inducing arthritis in mice and studying the afflicted muscles, we could measure the production of reactive oxygen species by these two sources. However, mitochondria and NOX2 appeared not to produce more reactive oxygen species in

muscles that were affected by arthritis. Nevertheless, when we treated the arthritic mice with a novel drug that can clear reactive oxygen species (a new type of antioxidant), the muscles that were affected by arthritis became as strong as healthy control muscles. The drug is called EUK-134 and can clear reactive oxygen species from mitochondria and NOX2. These results were even more interesting when we found out that the production of the body's own antioxidants such as SOD2 and catalase, were increased in the muscles from the arthritic mice. Catalase was especially found more at the subcellular locations near the mitochondria that produce reactive oxygen species. EUK-134 has a similar function as that of SOD2 and catalase. Thus, although the arthritic mouse's antioxidant capacity of their muscles was increased and the mitochondrial and NOX2 production of reactive oxygen species was decreased, extra supplementation with EUK-134 could recover their muscle force. This shows that the source that causes oxidative stress in arthritic muscles is different than the main considered sources of reactive oxygen species (i.e. the mitochondria and NOX2).

To conclude, muscle weakness in rheumatoid arthritis patients is partly the effect of damage on important proteins of the muscles that regulate force. To effectively counteract muscle weakness caused by oxidative stress in RA, it is needed to have a good understanding of the sources and scavengers of reactive oxygen species inside the muscles. Novel drugs that specifically target oxidative stress at locations close to the important proteins can have the potential to improve muscle force in rheumatoid arthritis. Thereby the results of this study can ultimately improve the quality of life of rheumatoid arthritis patients.

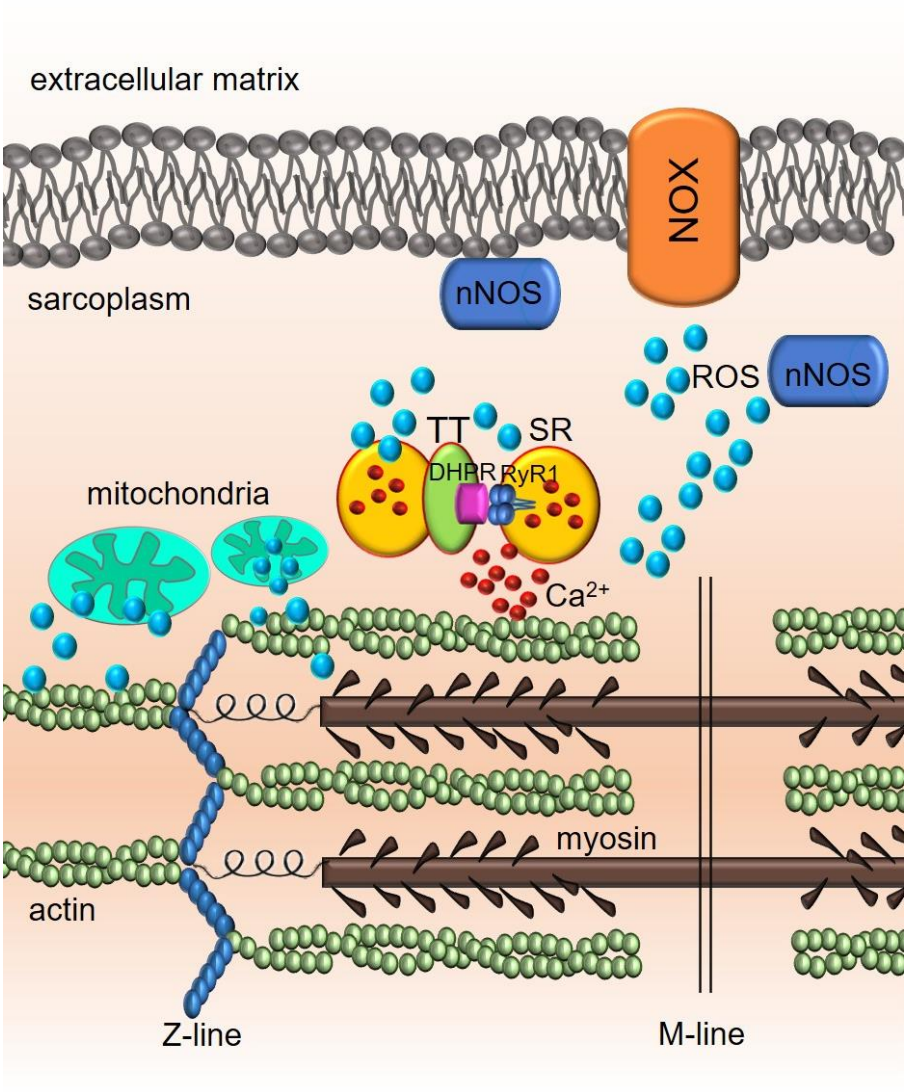

Illustration for the popular summary: oxidative stress can cause damage on important proteins that regulate muscle force. Two of the most important proteins that regulate muscle force are the ryanodine receptor (RyR1) and actin. The ryanodine receptor is the channel that regulates calcium release from the place where it is stored: the sarcoplasmic reticulum (SR). Calcium enables myofibrillar force production and actin (green filaments, composed of many actin molecules) is an important protein structure of the myofibrils. The myofibrils form the force-producing units of the muscle. Damages on RyR1 and actin can be caused by reactive molecules called reactive oxygen species (ROS, blue balls). They are produced at specific locations inside the muscle by proteins such as the mitochondria (aquamarine) and NOX (orange). These damages cause decreased muscle force. Counteracting such damage can improve the normal function of the muscle in diseases where increased oxidative stress plays a role such as rheumatoid arthritis.

“Cogito, ergo sum”

- *René Descartes (Discours de la méthode)*

-

ABSTRACT

Muscle weakness is a common comorbidity of several severe diseases which results in a reduced independence and quality of life and for the afflicted patients. For instance, patients with rheumatoid arthritis (RA), a disease characterized by a chronic inflammation of the joints, commonly report of muscle weakness as a complication. Muscle weakness is the result of reduced muscle size and intramuscular impairments (i.e. intrinsic muscle dysfunction). However, the mechanisms whereby a chronic inflammatory condition as RA leads to muscle weakness is not fully understood.

Oxidative stress due to an imbalanced production and scavenging of reactive oxygen species (ROS), is associated with intrinsic muscle dysfunction in RA. It can cause oxidative post translational modifications (oxPTMs) on RyR1 and actin which regulate muscle force production. In paper I, we show that mice with arthritis and patients with RA have a significantly decreased muscle strength which can be attributed to oxidative post-translational 3-nitro tyrosine (3NT) and malondialdehyde (MDA) modifications on actin. Combined with the results of paper II, we could conclude that the oxPTMs are introduced on specific hotspots regions of actin which impair actin-myosin cross-bridge formation and decrease actin polymerization. In addition to actin, oxidative stress on the ryanodine receptor 1 (RyR1) is associated increased RyR1 open-probability and Ca^{2+} leak which can ultimately lead to muscle weakness. In paper III we showed that specific 3NT and MDA modifications on RyR1 increase the channel's open probability and lead to dissociation of the RyR1 stabilizing protein FKBP12. The results together stress the need to study how muscle weakness caused by oxidative stress can be counteracted. Therefore, we in paper IV identified the effect of arthritis on the sources and scavengers of ROS in skeletal muscle. In paper IV we showed that while the expression of ROS scavengers SOD2, catalase and GPX1 was increased, treatment of mice with the SOD/catalase mimetic EUK-134 significantly restored muscle force. All results together stress the importance of targeted therapy against oxidative stress-induced muscle weakness in RA.

LIST OF SCIENTIFIC PAPERS

I. **Oxidative hotspots on actin promote skeletal muscle weakness in rheumatoid arthritis.**
JCI Insight, 2019, 5. piii:126347. doi:1172/jci.insight.126347

MAARTEN M STEINZ, Malin Persson, Bejan Aresh, Karl Olsson, Arthur J. Cheng, Emma Ahlstrand, Mats Lilja, Tommy R. Lundberg, Eric Rullman, Kristina Ängeby Möller, Katalin Sandor, Sofia Ajeganova,Takashi Yamada, Nicole Beard, Björn C.G. Karlsson, Pasi Tavi, Ellinor Kenne, Camilla I. Svensson, Dilson E. Rassier, Roger Karlsson, Ran Friedman, Thomas Gustafsson, and Johanna T. Lanner

II. **Force generated by myosin cross-bridges is reduced in myofibrils exposed to ROS/ RNS**
American Journal of Physiology Cell Physiology, 2019, https://doi.org/10.1152/ajpcell.00272.2019

Malin Persson, MAARTEN M STEINZ, Håkan Westerblad, Johanna T Lanner and Dilson E Rassier

III. **Oxidative MDA and nitration modifications on RyR1 lead to higher open probability and FKBP12 dissociation**
Manuscript

MAARTEN M STEINZ; Nicole Beard; Johanna T. Lanner

IV. **The role of ROS sources and scavengers in skeletal muscle of mice with arthritis**
Manuscript

MAARTEN M STEINZ*, Michaeljohn Kalakoutis*, Anna-Lena Boller, Theresa Mader, George G. Roodney, Pasi Tavi, Johanna T. Lanner

CONTENTS

LIST OF ABBREVIATIONS

AA	Arachidonic Acid
ACPA	Anti-Citrinullated Protein Antibodies
ACR	American College of Rheumatology
AIA	Adjuvant Induced Arthritis
CaM	Calmodulin
CaMBD	CaM Binding Domain
CaMKII	Calmodulin-Dependent Protein Kinase II
CFA	Complete Freund's Adjuvant
CIA	Collagen Induced Arthritis
CI-IV	Mitochondrial Complex I-IV
Cn	Copernicium
CoQ	Co-enzyme Q10
CSA	Cross-Sectional Area
CsMS	Cesium Methane Sulfonate
Cu	Copper
D	Aspartic Acid
DAS	Disease Activity Score
DHPR	Dihydropyridine Receptor
DMARDs	Disease-Modifying Anti-Rheumatic Drugs
DMF	Dimethyl Fumarate
DNP	Carbonylation
DR2	Divergent Region Two
DTT	Dithiothreitol
E	Glutamic Acid

ECC	Excitation-Contraction Coupling
EDL	Extensor Digitorum Longus
eNOS	Endothelial NOS
EULAR	European League Against Rheumatoid Arthritis
F-actin	Filamentous Actin
f_{app}	Rate of Cross Bridge Attachment
FCB	Force per Cross Bridge
FDB	Flexor Digitorum Brevis
FKBP12	FK506-binding Protein 12
FMN	Flavine Mononucleotide
g_{app}	Rate of Cross Bridge Detachment
GPX	Glutathione Peroxidases
GSH	Glutathione
GSSG	Glutathione Disulfide
H	Histidine
H_2O_2	Hydrogen Peroxide
HMOX	Heme Oxygenase
iNOS	Inducible NOS
JSol	Junctional Solenoid
K	Lysine
$LOO^{\bullet}$	Lipid Peroxide Radical
LOOH	Lipid Hydroperoxide
MDA	Malondialdehyde
Mn	Manganese
N	Asparagine
n_{CB}	Number of Cross Bridges
nNOS	Neuronal NOS

NOS	Nitric Oxide Synthases
NOX	NADPH Oxidases
NQO	NAD(P)H Dehydrogenases
NTD	N-terminal Domain
$O_2^{\bullet-}$	Superoxide
$ONOO^-$	Peroxynitrite
oxPTM	Oxidative Post-Translational Modifications
PBS	Phosphate Buffered Saline
PKA	Protein Kinase A
PLA2	Phospholipase 2
PRX	Peroxiredoxins
pVSD	Pseudo Voltage Sensitive Domain
Q	Glutamine
Q_i	Reduction Side of Co-enzyme Q
Q_o	Oxidation Side of Co-enzyme Q
R	Arginine
RA	Rheumatoid Arthritis
RET	Reverse Electron Transport
RMSF	Root Mean Square Fluctuations
roGFP	Reduction-oxidation Sensitive Green Fluorescent Protein
ROS	Reactive Oxygen Species
RY1&2/3&4	RyR Repeat Domains 1&2/3&4
RyR1	Ryanodine Receptor 1
SASA	Solvent-Accessible Surface Area
SCLP	Shell-Core Linker Peptide
SD	Subdomain
SERCA	Sarcoplasmic Reticulum Ca^{2+} ATPase

SIN-1	5-amino-3-(4-morpholinyl)-1,2,3-oxadiazolium Chloride
SNO	S-Cysteine-Nitrosylation
SOD	Superoxide Dismutase
SPRY	spIA Kinase and RyR Domain
SR	Sarcoplasmic Reticulum
TaF	Thumb and Forefinger
TRX	Thioredoxins
TT	T-Tubulus
Y	Tyrosine
Zn	Zinc
3NT	3-Nitro Tryosine
6-TM	Six-Transmembrane

1 BACKGROUND

1.1 INTRODUCTION

Muscle weakness is a risk factor for negative health outcomes associated with loss of independence and reduced quality of life since most of our daily activities require muscular work (1). Muscle weakness is present in many diseases, including rheumatoid arthritis (RA) (2-6), cancer (7) and sepsis (8), which are diseases also associated with an increased (chronic) local or systemic inflammation. Muscle weakness can be the combined result of reduced muscle size (atrophy) and intramuscular impairments (intrinsic muscle dysfunction). Interference with the excitation-contraction coupling (ECC), the force producing machinery (i.e. cross-bridge cycling), and/or accumulation of non-contractile tissue (e.g. fat, fibrosis) can all be contributing factors to intrinsic muscle dysfunction that reduces the capacity of the muscle to generate power. Disease-induced muscle weakness is commonly attributed to reduced muscle mass (9-11), however, research from our group and others has shown that a decrease in muscle mass cannot solely explain muscle weakness associated with a chronic inflammatory disease (2, 3, 12). In fact, the mechanisms whereby inflammation leads to muscle weakness is still unclear.

The aim of this thesis is to define the molecular mechanisms behind muscle weakness associated with the chronic inflammatory condition of RA, which ultimately could lead to improve the quality of life of patients suffering from muscle weakness and fatigue.

1.1.1 Rheumatoid arthritis

Rheumatoid arthritis is one of the most common chronic inflammatory diseases and affects primarily women in the age of 40-50 years (13-15). The disease is characterized by a chronic inflammation of the joints with systemically elevated levels of e.g. circulating cytokines (e.g. tumor necrosis factor α (TNF-α), interleukine-6 (IL-6), monocyte chemoattractant protein 1 (MCP1), and interleukin-1 (IL-1))(16, 17), autoantibodies to immunoglobulin G (Rheumatoid Factor, RF) and autoantibodies against citrinullated proteins (anti-citrinullated protein antibodies, ACPA's) (15-18). When RA is left untreated it will ultimately lead to severe damage and destruction of the joints (15). It has been shown that the quality of life and work productivity in RA patients is significantly reduced in association with physical limitations (1). Patient with RA indeed suffer from muscle weakness and fatigue, including a reduction in muscle strength without corresponding loss of muscle mass (2),(3),(4, 12, 19-21). Moreover, a decreased physical ability in RA is associated with elevated levels of pro-inflammatory cytokines as IL-1β and IL-6 (18). Up until today however, little molecular insight is available on how a chronic inflammation as RA induces muscle weakness. In this thesis we elucidated the skeletal muscle capacity in mice afflicted with arthritis and in patients with RA.

1.2 SKELETAL MUSCLE

1.2.1 The structure of the skeletal muscle

There are three different types of muscle in the body: cardiac muscle, smooth muscle and skeletal muscle. The human body consist of ~35-40% of skeletal muscle relative to body weight (22). Skeletal muscles are essential for our ability to move and one of its major purposes is to produce force (23, 24). A given muscle is made of hundreds to thousands of multinucleated muscle fibers bundled together (**Figure. 1**) (23, 24). The muscle bundles and the muscle itself are surrounded by connective tissue called the perimysium and epimysium, respectively (24). Looking further into the structure of each muscle fiber, it can be observed that it consists of thousands of myofibrils (23), which are repeats of thick and thin filaments that form the functional unit called the sarcomere (**Figure. 2**) (23). The sarcomere's thick filaments consist of myosin and other proteins such as titin (25), whereas the thin filaments are composed of troponin and tropomyosin that are wrapped around the centrally located actin filament (F-actin) (23, 25). The F-actin filament is composed of actin monomers (G-actin) (26).

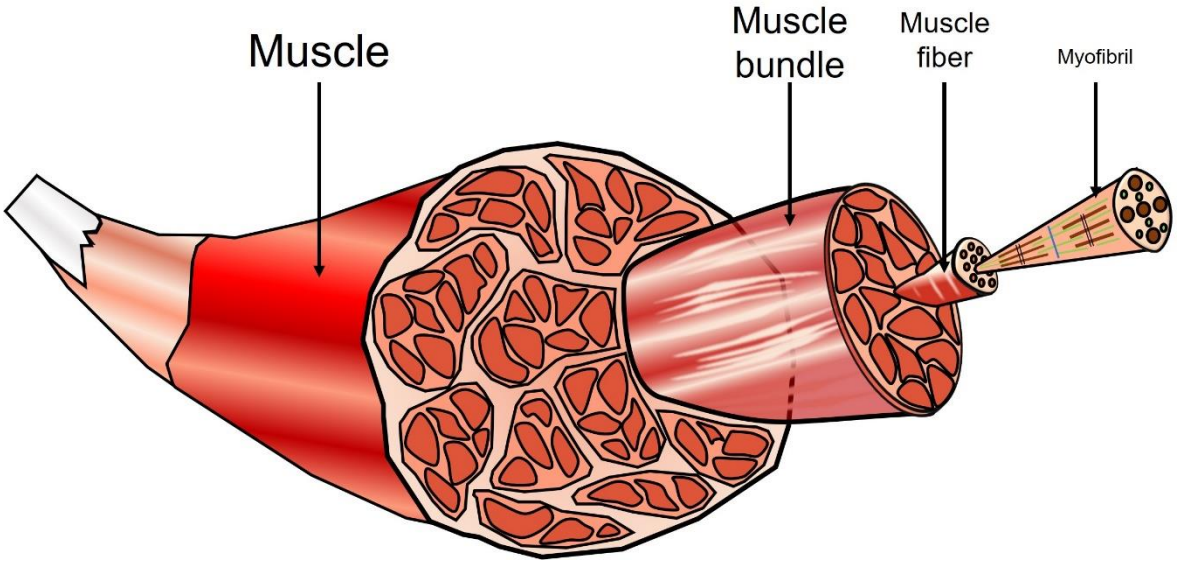

Figure 1. Illustration of the composition of a muscle. A muscle is made of muscle bundles that each consist of hundreds to thousands of muscle fibers (here only illustrated a few for simplicity of the picture). Each muscle fibers contains many myofibrils which are repeats of many well-organized sarcomeres.

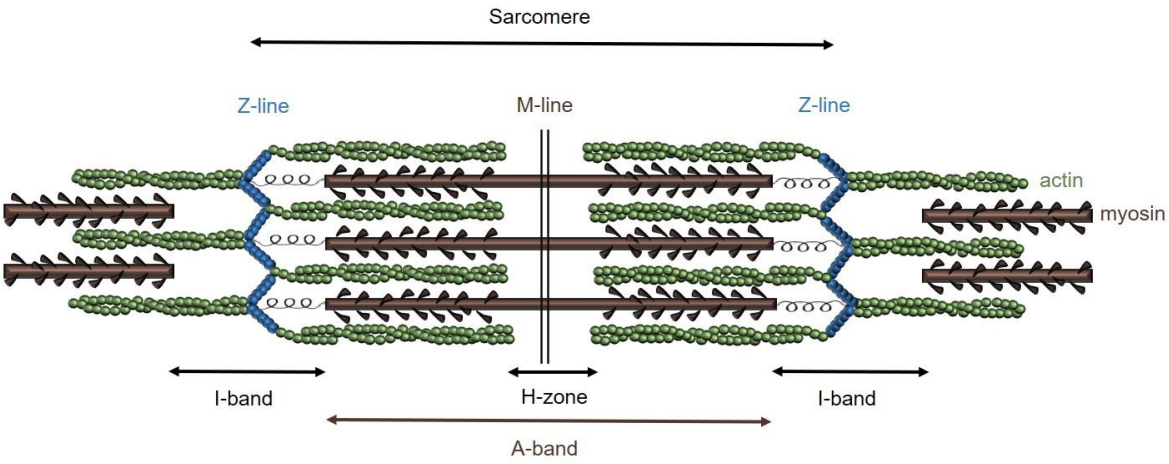

Figure. 2 The organization of the muscle's sarcomere. Each sarcomere spans from one z-line (shown in blue) to the other z-line and is composed of thick filaments that contain myosin (shown in brown), and thin filaments that contain as actin (shown in green). The middle of the sarcomere is the M-line. Other bands that can be distinguished are the I-band, A-band and H-zone as illustrated above. The interaction of actin and myosin results in force production of the muscle. Repeats of sarcomeres form a myofibril, which is one of the smallest functional units that force can be measured on *in-vitro*.

1.2.2 Excitation-contraction coupling and force production

Skeletal muscle force is generated through the excitation-contraction coupling (ECC) and the interaction of contractile proteins in the force producing machinery (cross-bridge cycling) (**Figure. 3**) (27). The concept of ECC was first postulated in 1952 by Alexander Sandow (28). When an action potential is propagated to the t-tubules of the SR it triggers the voltage-dependent dihydropyridine receptor (DHPR) activation in the sarcolemma. DHPR mechanically interacts with the ryanodine receptor 1 (RyR1) which is in the membrane of the sarcoplasmic reticulum (SR) inside the muscle cell (29). Activation of the DHPR causes the RyR1 opening and the Ca^{2+} is released from the SR into the cytoplasm (29). The intracellular Ca^{2+} concentration ($[Ca^{2+}]_i$) increases and Ca^{2+} interacts with troponin causing displacement of the tropomyosin filaments along actin. This opens the site where the myosin head can bind to the actin filament. During the power stroke in the cross-bridge cycling, the myosin head will change its conformation and pull in actin, which thereby enables force production (25, 30). Ca^{2+} is pumped back into the SR by the SR Ca^{2+} ATPase (SERCA) which allows the muscle to relax (19, 29). The $[Ca^{2+}]_i$-force relationship is sigmoidal which reaches a plateau where maximum force is reached at high $[Ca^{2+}]_i$ (31). In mouse muscle fibers under resting conditions the $[Ca^{2+}]_i$ is ~50-100 nM and when activated, $[Ca^{2+}]_i$ increases to ~1 μM (31).

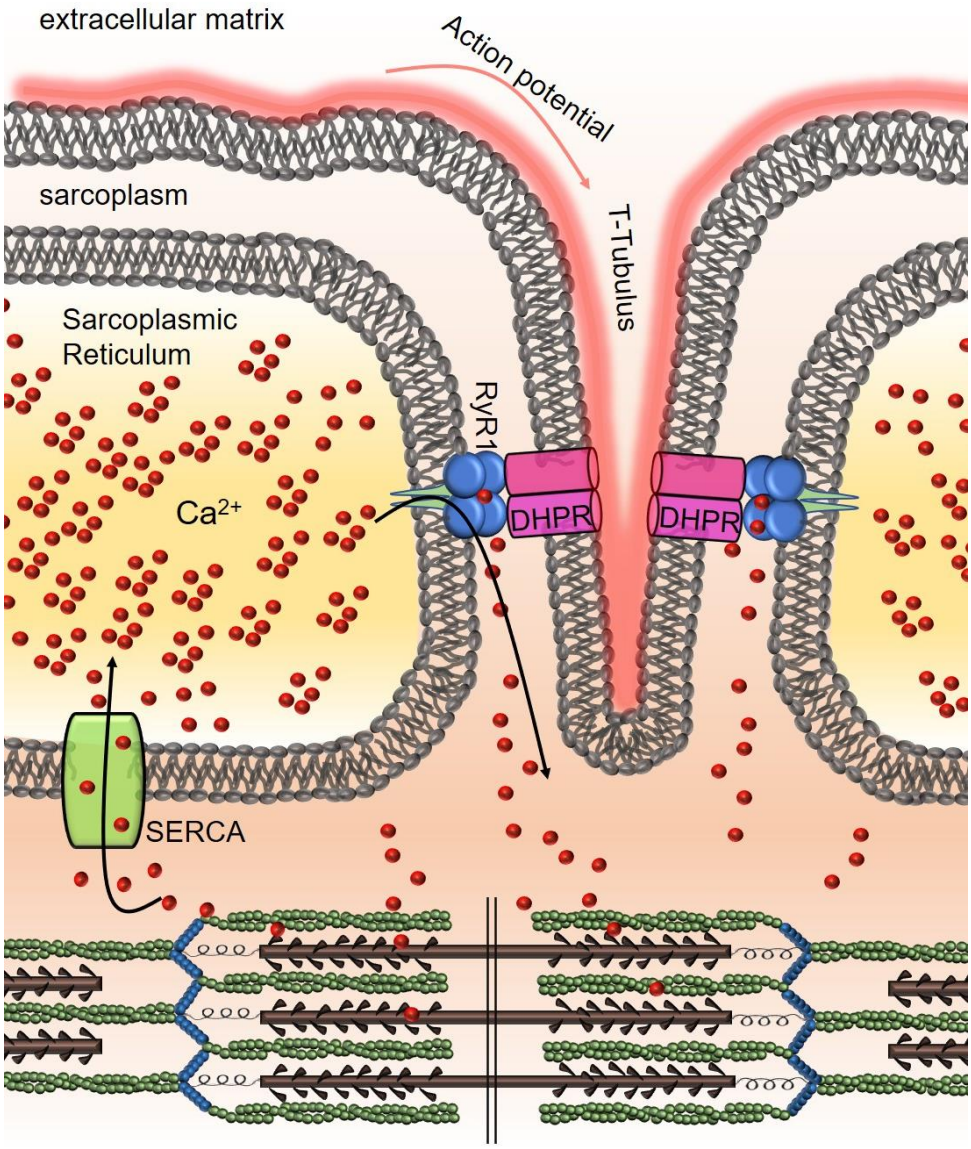

Figure 3. Illustration of excitation-contraction coupling (ECC). ECC starts with an action potential that reaches the t-tubules of a muscle fiber. This causes mechanical interaction of dihydropyridine receptors (DHPR, shown in pink) with the ryanodine receptor 1 (RyR1, shown in blue) of the sarcoplasmic reticulum (SR). Thereby Ca^{2+} will be released via RyR1 into the sarcoplasm which enables actin-myosin cross-bridge formation and thereby force production of the muscle. Ca^{2+} is pumped back into the SR by the SR Ca^{2+} ATPase (SERCA).

1.2.3 Skeletal muscle weakness associated with RA

A decrease in muscle mass in patients with a chronic inflammatory disease as RA, is associated with a decrease in muscle strength (11, 32, 33). However, Helliwell & Jackson showed already in 1994 that a decrease in fore-arm muscle mass of RA patients can only explain 40% of the decrease in fore-arm grip strength (12). Later, more studies have shown that muscle weakness due to a chronic inflammation cannot solely be explained by a decrease in muscle mass (2),(3),(4, 19-21). Based on these findings, it was postulated that intrinsic muscle dysfunction may be an important contributor to muscle weakness accompanying RA (19). More specifically, they can be an effect of (i) decreased Ca^{2+} release from the SR by

RyR1, (ii) decreased sensitivity of myofibrils to Ca^{2+} and (iii) a decreased ability of actin and myosin to generate myofibrillar force (19). Concerning the latter in more detail: myofibrillar isometric force production depends on: (a) the number of actin-myosin cross bridges (n_{CB}), (b) the force per cross bridge (F_{CB}), (c) the rate of cross bridge attachment (f_{app}) and (d) the rate of cross-bridge detachment (g_{app}) (34, 35).

1.3 OXIDATIVE STRESS

Oxidative stress is a term to describe to maladaptive effects of an imbalanced production of reactive oxygen and nitrogen species (ROS) at a specific subcellular place, time and amount (36). ROS can be free radicals, i.e. superoxide ($O_2^{\bullet-}$), peroxynitrite ($ONOO^{\bullet-}$) and hydroxyl radical ($OH^{\bullet}$), or non-free radicals, i.e. hydrogen peroxide (H_2O_2) which can form $OH^{\bullet}$ (37). ROS can cause oxidative post-translational modifications (oxPTM) of amino acid residues of proteins. Oxidative stress has been shown to be part of the pathophysiology of RA (2, 3, 38-40).

1.3.1 Oxidative post-translational modifications

OxPTM on skeletal muscle proteins caused by oxidative stress can be reversible or stable changes of amino acids. There are several types of oxPTMS as nitrosylation (SNO), carbonylation (DNP), nitration (NT) and malondialdehyde adducts (MDA). Nitrosylation is an oxPTM occurring mostly on cysteine residues, i.e. S-nitrosylation, which can be reversed enzymatically by e.g. glutaredoxin (GPX) or thioredoxin (TRX) (41). On the other hand, carbonylation, nitration and addition of a malondialdehyde (MDA) adduct are more stable changes to amino acids (41-45). Hallmarks of both nitration and MDA adducts have been found in RA patients (38, 39) and rodents with arthritis (2, 3). Due to the stability of nitration and MDA adducts, progressive protein damage may occur (46). It is for these reasons we have focused on these two types of modifications in relation with oxidative stress and muscle weakness associated with RA.

1.3.2 Tyrosine nitration

The amino acid tyrosine (Y) contains a phenol group that plays a central role in nitration. One of the first biological evidences for 3-nitrotyrosines (3NT) (**Figure. 4**) came from Ohshima et al. in 1990, showing that rats had increased levels of nitrated proteins in their plasma after injection of the nitrating compound tetranitromethane (47). A push for research on nitration of tyrosine residues in a biological setting came after Beckman *et al.* showed that $ONOO^-$ is a highly reactive intermediate that can be formed during the biological reaction of NO with $O_2^{\bullet-}$ (48). The formation reaction of $ONOO^-$ has a fast rate constant between 7.5 and 21 x 109 M^{-1} s^{-1} (49). It has later become clear that the biological formation of 3NT happens in multiple steps (43). ROS can promote the formation of a tyrosine radical ($Tyr^{\bullet}$) which can react with $ONOO^-$ derived radicals, leading to addition of a nitro-group on the third C position of the phenol ring of tyrosine (43). Increased 3NT levels have been observed on skeletal muscle actin of mice and rats with arthritis (2, 3). $Tyr^{\bullet}$ can also react with another $Tyr^{\bullet}$ to form 3, 3'-dityrosine (43) and it has been shown that nitrated proteins can cause formation of protein

aggregates (50). Actin aggregates have previously been found in rat models of high oxidative stress, as well as in a rat model of arthritis (3, 51). In addition to actin, RyR1 contains many tyrosine residues which could be susceptible for nitration, and 3NT modifications have been found on the RyR1 complex in mice with arthritis (2).

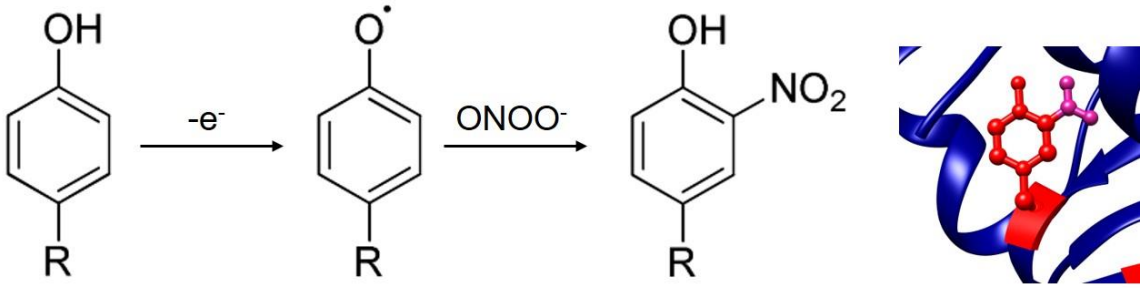

Figure 4. Tyrosine nitration (3-NT). From left to right: tyrosine, tyrosine radical, 3-nitrotyrosine (3NT) and an illustration of 3NT within a 3-dimensional protein crystal structure (NO_2, +46 Da, shown in pink).

1.3.3 Malondialdehyde adducts

MDA is a reactive aldehyde which can react with basic amino acids such as Histidine (H), Lysine (K), Arginine (R), Glutamine (Q) and Asparagine (N) (**Figure. 5**) (42, 52). MDA is generated enzymatically during the synthesis of pro-inflammatory eicosanoids (i.e. thromboxane A2), and non-enzymatically during lipid peroxidation (42). Lipid peroxidation takes place in three steps and in the first initiation step, a lipid radical ($L^{\bullet}$) is formed due to the reaction of ROS with the hydrogen of the allyl group next to the carbon-carbon double bound of an unsaturated lipid. Then, in the propagation step, $L^{\bullet}$ reacts with oxygen and forms a lipid peroxide radical ($LOO^{\bullet}$). $LOO^{\bullet}$ reacts with another lipid molecule to form a new $L^{\bullet}$ and lipid hydroperoxide (LOOH). In the terminating step $LOO^{\bullet}$ from the propagation step will react with an antioxidant such as vitamin E to form a non-radical LOOH (42). $LOO^{\bullet}$ can alternatively cyclize to and endoperoxide which, by cleavage, will form MDA. Intriguingly, increased levels of auto-antibodies against MDA-modified proteins have been found in serum and the synovium from RA patients (38, 39, 53).

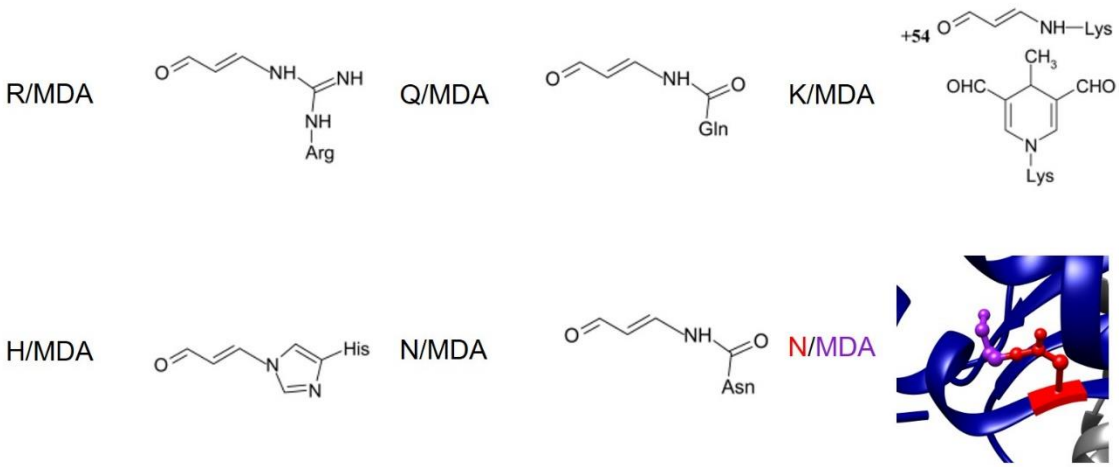

Figure 5. Malondialdehyde (MDA) adducts on arginine, glutamine, lysine, histidine and asparagine. From left to right top row: Arginine-MDA (R/MDA), Glutamine-MDA (Q/MDA), Lysine-MDA (K/MDA). From left to right bottom row: Histidine-MDA (H/MDA), Asparagine (N/MDA) and illustration of N/MDA within a 3-dimensional protein crystal structure (C3H3O, +54 Da, shown in pink). The proposed MDA modifications are adapted from Zhao et al. (52).

1.3.4 Effects of oxidative post-translational modifications on skeletal muscle proteins

The effect of oxPTM on skeletal muscle force production have been examined by incubating muscle with various oxidants. Hydrogen peroxide (H_2O_2) (54), peroxynitrite ($ONOO^-$) and the NO and $O_2^{-\bullet}$ donor 5-amino-3-(4-morpholinyl)-1,2,3-oxadiazolium chloride (SIN-1) (55) have been used to study the direct effects of oxidative stress on skeletal muscle force production. SIN-1 forms $ONOO^-$ at a linear relation to its original concentration (56). Sustained incubation of skeletal muscle fibers with H_2O_2 results in decreased force production and the force decline was diminished after adding the reducing agent DTT (54). A study by Dutka et. al in 2011(55), showed that force of skinned muscle fibers was decreased after addition of ONOO- or SIN-1. The reduced force of single muscle fibers after SIN-1 incubation has been attributed to a decline in Ca^{2+} sensitivity of the myofibrils (55, 57). These studies report about observed changes in force production in the presence of oxidative agents. However, they do not explain the underlying molecular details of $ONOO^-$ -induced 3NT and MDA modifications on contractile muscle proteins that are essential for force production. In this thesis, the functional effects of introducing 3NT and MDA modifications were clarified in relation to the force production by myofibrils, the polymerization of actin and the open probability of RyR1.

1.3.5 Oxidative modifications on myofibrils and actin

The myofibrils are the force-generating machinery of the muscle. A major component of the myofibrils is the centrally located actin filament. Previous studies have shown that actin is a primary target for oxidative 3NT modifications (58, 59) which is associated with muscle weakness in arthritis (2, 3). Moreover, oxPTMs on actin have been found in association with Alzheimer's disease (60), Freidrich's ataxia (61), and inflammation and pain (62). Actin

filaments have a helical structure with a fast (barbed) and slow (pointed) end. The actin filament is formed through polymerization of actin monomers (G-actin) (**Figure. 6**). The structure of G-actin was first described in 1990 (63) and improvements in techniques that determine the crystal structure of a protein, have now given a detailed picture of what monomeric G-actin and its four subdomains look like 3-dimensionally (64, 65). G-actin polymerization to F-actin, is an allosteric process and is coupled to ATP hydrolysis (26, 66, 67). Assembly of ATP-bound G-actin at the barbed end, is followed by nucleotide hydrolysis and dissociation of ADP-bound G-actin at the pointed end (68). ADP-bound actin can undergo nucleotide exchange to form new ATP-bound actin that can bind to the barbed end of the actin filament again (66, 67).

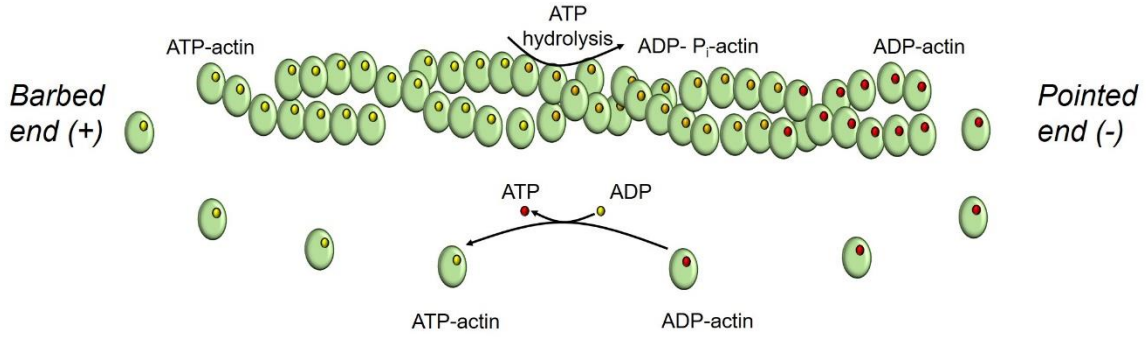

Figure 6. Illustration of actin-polymerization. Actin forms the centrally located filament of the thin filaments of the myofibrils' sarcomeres. The actin filament (F-actin), as illustrated above, is composed of many actin monomers (G-actin). The polymerization of G-actin to F-actin is a continuous process of addition of ATP-actin on the barbed end of the filament and dissociation of ADP-actin on the pointed end of the filament. ATP hydrolysis to ADP-Pi actin happens when ATP-bound actin moves towards the pointed end. ADP-actin can subsequently exchange ADP for ATP so that it can bind the filament again.

Due to the continuous process of polymerization, the actin filament is polymorphic and the G-actin monomers within an actin filament are in contact with neighboring actin monomers and with myosin (69, 70). It is for these reasons that protein modifications in the form of oxPTMs are likely to affect actin polymerization and myofibrillar force production. The direct effects of oxidative 3NT and MDA modifications on myofibrillar force and actin polymerization have up until today not been elucidated and neither is it known if they can cause muscle weakness in muscles affected by RA. We studied the effects of oxPTMs 3NT and MDA on myofibrillar force and actin polymerization in muscles from mice with arthritis and patients with RA.

1.3.6 Oxidative modifications on RyR1

Muscle force production is Ca^{2+} dependent and increases with increased Ca^{2+} release (71). Thus, for myofibrils to be able to contract, Ca^{2+} release from the SR is needed. The RyR1 complex tightly regulates Ca^{2+} release from the SR(72). Many researchers have aimed to unravel the structure of RyR1(73-77) and thanks to improved methodology with cryo-EM, more details of crystal structure of RyR1 have become available (73, 74, 78). RyR1 has a

large cytosolic shell and relatively small trans membranous pore region with each RyR1 monomer containing 21 specific subdomains (73, 74).

RyR1 has gained a lot of interest when it comes to understanding the functional effects of post-translational modifications on RyR including phosphorylation, nitrosylation and other oxidative modifications (7, 45, 79, 80). There are three isoforms of RyR (RyR1, 2 &3) of which the ~2.2MDa big homotetrameric and in the skeletal muscle main expressed isoform is RyR1 (29, 72). The expression of RyR1 in skeletal muscle was found in 1989 by Takeshima *et al. (81)* and Zorzato *et al.* in 1990 (82). RyR1 forms a super-complex with other regulatory proteins, such as calmodulin (CaM) and the FK506-binding protein 12 (FKBP12) (29). In addition, other ions and proteins are known to regulate the activity of RyR1, such as Ca^{2+}, Mg^{2+}, calmodulin-dependent protein kinase II (CaMKII) and protein kinase A (PKA) (29). Many studies have shown that dissociation of FKBP12 in association with increased levels of oxPTMs on the RyR1 complex (7, 29, 83-85). However, only a few studies have been able to directly link a specific modified amino-acid residue to altered RyR1 gating (86-88). One post-translational modification on RyR1 that indeed can alter the function of RyR1, is nitrosylation of Cystein3635, which has been shown to activate the RyR1 complex (88, 89). In addition, phosphorylation of Ser2843 can enhance RyR1 activity through dissociation of FKBP12 from the receptor (29, 90-93). Mass spectrometry experiments of this thesis allowed for the identification of the exact amino acids of RyR1 that are susceptible to 3NT and MDA modifications.

Increases in post-translational modifications on RyR1 have been shown to make the channel less stable which may result in Ca^{2+} leak and less Ca^{2+} release that in turn can contribute to muscle weakness (7). For example, increased RyR1 nitrosylation leading to RyR1 channel leak has been associated with reduced grip-strength in mdx mice, a mouse-model of Duchenne muscular dystrophy (85). In addition, a higher level of nitrosylated RyR1 along with increased Ca^{2+} sparks and decreased muscle force have been found in aged mice as compared to young control mice (80). Moreover, increased oxidative stress (3NT, MDA) of RyR1 has been linked to decreased muscle force production in RA (2). Thus, although associated to muscle weakness in RA, it is not entirely understood how 3NT and MDA modifications affect the gating properties of RyR1. In this thesis, we directly measured the effects of introducing 3NT and MDA modifications on RyR1 open probability with single channel recordings in lipid bilayers.

1.4 SOURCES & SCAVENGERS OF ROS IN SKELETAL MUSCLE

Although oxidative stress is associated with RA, it is up until today not clear how arthritis affects the sources and scavengers of ROS in skeletal muscle and how that causes oxidative stress. Mitochondria, NADPH oxidases (NOX) and nitric oxide synthases (NOS) have all been associated with ROS production in RA-induced muscle weakness (19). The scavenging of ROS originating from these sources is facilitated by ROS scavengers such as SOD2, catalase and GPX1 (37).

1.4.1 Mitochondria as a source of ROS

Mitochondria are organelles that are present in skeletal muscle and are the main producer of energy in the form of ATP (94). They consist of an inner and an outer membrane surrounding the intermembrane space and mitochondrial matrix (94). The inner membrane holds a lot of proteins such as the mitochondrial protein complexes (I, II, III, IV and V), which form an electron transport chain to transport protons to the intermembrane space (94). The generated proton gradient (protonmotive force) is used by complex V for the synthesis of ATP. During electron transport, oxygen is consumed by complex I, III and IV, and therefore these sites in the mitochondria are known sources of ROS, especially for $O_2^{\bullet-}$ formation, in skeletal muscle (95). The complexes can produce $O_2^{\bullet-}$ through one-electron transfer from a prosthetic group of a mitochondrial complex to O_2 (96). Complex I and III are considered the two major sites of $O_2^{\bullet-}$ production in the mitochondria (**Figure. 7**) (96, 97).

Complex I (CI) is the first complex of the electron transport chain (ETC) and transfers protons from NADH to the mitochondrial intermembrane space. Oxidation of NADH causes electrons to be transferred to co-factor flavine mononucleotide (FMN) of CI which transfers the electrons to co-enzyme Q10 (CoQ). O_2 is likely to be accessible for FMN and CoQ which make these two electron carriers likely to cause $O_2^{\bullet-}$ production (96). Already in 1977 it was shown that isolated CI produces $O_2^{\bullet-}$ through fully reduced FMN and the proportion of reduced FMN is determined by an increase in [NADH] (98). Therefore, the ratio of ratio NADH/ NAD^+ may determine the rate of $O_2^{\bullet-}$ by CI. An increase in [NADPH] has been hypothesized to be an effect of inhibition of respiration, mitochondrial damage or mutations, ischemia, loss of cytochrome c or low ATP demand and consequent low respiration rate (96). Other mechanisms of $O_2^{\bullet-}$ production by CI have been described, e.g. $O_2^{\bullet-}$ formation by reversed electron transport (RET) (96). RET occurs when electrons reduce the CoQ pool which in the presence of a significant protonmotive force transfers electrons back from $CoQH_2$ to FMN of CI. The site of CI that produces $O_2^{\bullet-}$ during RET is however still unclear.

Complex III (CIII) is the third complex of the ETC which receives electrons from $CoQH_2$ (95). The catalytic subunit of CIII consists of cytochrome b, c and an iron-sulfur center (95). There are two interaction sides of CIII for CoQ: the oxidation side (Q_o) and reduction side (Q_i) (95). When Q_i is inhibited with antimycin and when supplied with $CoQH_2$, CIII is known to produce $O_2^{\bullet-}$ (96). However, $O_2^{\bullet-}$ formation by complex III in physiological conditions is supposedly negligible compared to CI (96).

Mitochondrial dysfunction and altered specific mitochondrial gene expression have been associated with arthritis (18, 99, 100). Analysis of multiple microarray gene expression studies have indicated a differential expression of nuclear encoded genes of the mitochondrial complexes associated with mitochondrial dysfunction in the synovium of RA patients (100). Whether these observations are also valid for muscles affected by arthritis and if it leads to increased mitochondrial ROS production is not yet fully understood. In this thesis, the ROS production by mitochondria was measured in muscles afflicted with arthritis by using genetically encoded ROS probes specifically targeted towards the mitochondria.

1.4.2 ROS producers NOX2, NOS and PLA2

The identification of factors that are behind the decreased force production is an ongoing process, and other sources of ROS associated with RA-induced muscle weakness, e.g. NOX and NOS have previously been reviewed by our group (19). NOX can form $O_2^{\bullet-}$ by transferring electrons from NADPH to O_2 (101). Seven isoforms of NOX have been described of which NOX2 and NOX4 are present in skeletal muscles (101),(102). Other than NOX, NOS can produce ROS in skeletal muscle. NOS are homodimeric enzymes and three isoforms have been described; NOS1, NOS2 and NOS3, or also known as neuronal NOS (nNOS), endothelial NOS (eNOS) and inducible NOS (iNOS), respectively (103). NOS is forming NO, but in circumstances of sub-optimal L-Arginine concentrations, NOS can uncouple and cause the release of both NO and $O_2^{\bullet-}$ (103, 104), which can react to form $ONOO^-$. Thus, NOS is an inducer of NO, as well as $O_2^{\bullet-}$ and $ONOO^-$.

Increased levels of nNOS and NOX2 have been observed in muscles from rodent models of arthritis (2, 3). However, up until today the effects of those enzymes in the context of muscle weakness arising in RA has not yet been clearly determined. In addition to NOX2 and NOS, phospholipase 2 (PLA2) may also contribute to increased ROS production in association with arthritis. PLA2 hydrolyze phospholipids to arachidonic acid (AA) which is the main precursor for the formation of MDA both in the enzymatic and non-enzymatic pathway of MDA formation (42). Increased skeletal muscle ROS production by PLA2 has been ascribed to enhanced mitochondrial ROS production (105) or enhanced lipoxygenase-dependent ROS production (106). In the last paper of this thesis, the gene and protein expression for NOX2 were measured in skeletal muscles affected by arthritis in comparison with healthy control muscles. In addition, genetically encoded ROS probes targeted towards NOX2 were used to study the NOX2-specific ROS production in muscles affected by arthritis.

1.4.3 ROS scavengers SOD, catalase and GPX1

The scavenging of ROS in skeletal muscle happens through by a specialized antioxidant defense system in order to prevent oxidative damage. The term antioxidant has been defined as “any substance that delays or prevents the oxidation of a substrate” and there are both biological and dietary antioxidants (e.g. vitamin E, vitamin C and carotenoids) (37). The biological antioxidants can subsequently be divided into antioxidant enzymes and non-enzymatic antioxidants. Further in this thesis, we refer to the biological enzymatic antioxidants as ROS scavengers. Superoxide dismutases (SOD), catalase, and glutathione peroxidases (GPX) are considered as the primary scavengers of $O_2^{\bullet-}$ in skeletal muscle (37) (**Figure. 7**). Other ROS scavengers in skeletal muscle are thioredoxins (TRX), peroxiredoxins (PRX), heme oxygenases (HMOX) and NAD(P)H dehydrogenases (NQO)(37, 107).

There are three different isoforms of SOD (SOD1, SOD2 and SOD3) and they scavenge $O_2^{\bullet-}$ to H_2O_2. All SOD contain a metal ion in its catalytic site for the catalytic breakdown of $O_2^{\bullet-}$; SOD1 carry (Cu) or zinc (Zn); SOD2 carry manganese (Mn) and SOD3 carry copernicium

(Cn) or Zn (37, 108). Catalase scavenges H_2O_2 to H_2O plus O_2 and contains iron at its active site (37, 109). In addition to catalase, GPX is scavenging H_2O_2 and five different isoforms GPX have been described (37). GPX scavenges H_2O_2 through catalyzation of the reaction of glutathione (GSH) with H_2O_2 to glutathione disulfide (GSSG) and H_2O (37).

Although the specific location of SOD, catalase and GPX have been described, the exact subcellular localization in skeletal muscle is still not completely elucidated. Of the isoforms of SOD, SOD1 is thought to be localized in the cytosol and mitochondrial intermembrane space, SOD2 in the mitochondria and SOD3 is in the extracellular space (37, 108). Catalase, is known to be present in the peroxisomes of the skeletal muscles, an organelle that is metabolically linked and interacting with the mitochondria (110, 111). Of the five isoforms, GPX1 and GPX3 are expressed in all tissues including skeletal muscle, and GPX1 is specifically located in the cytosol and mitochondria (37). If the scavengers can change their position upon inflammation-induced oxidative stress is not known and whether their expression increases at a specific location where increased ROS production may happen is neither elucidated. In this thesis we looked at the expression of two of the main scavengers of $O_2^{\bullet-}$ and H_2O_2, i.e. SOD2 and catalase, in skeletal muscle, by super-resolution imaging with an airy scan confocal microscope and compared the expression and subcellular localization between muscles afflicted with arthritis and healthy muscles.

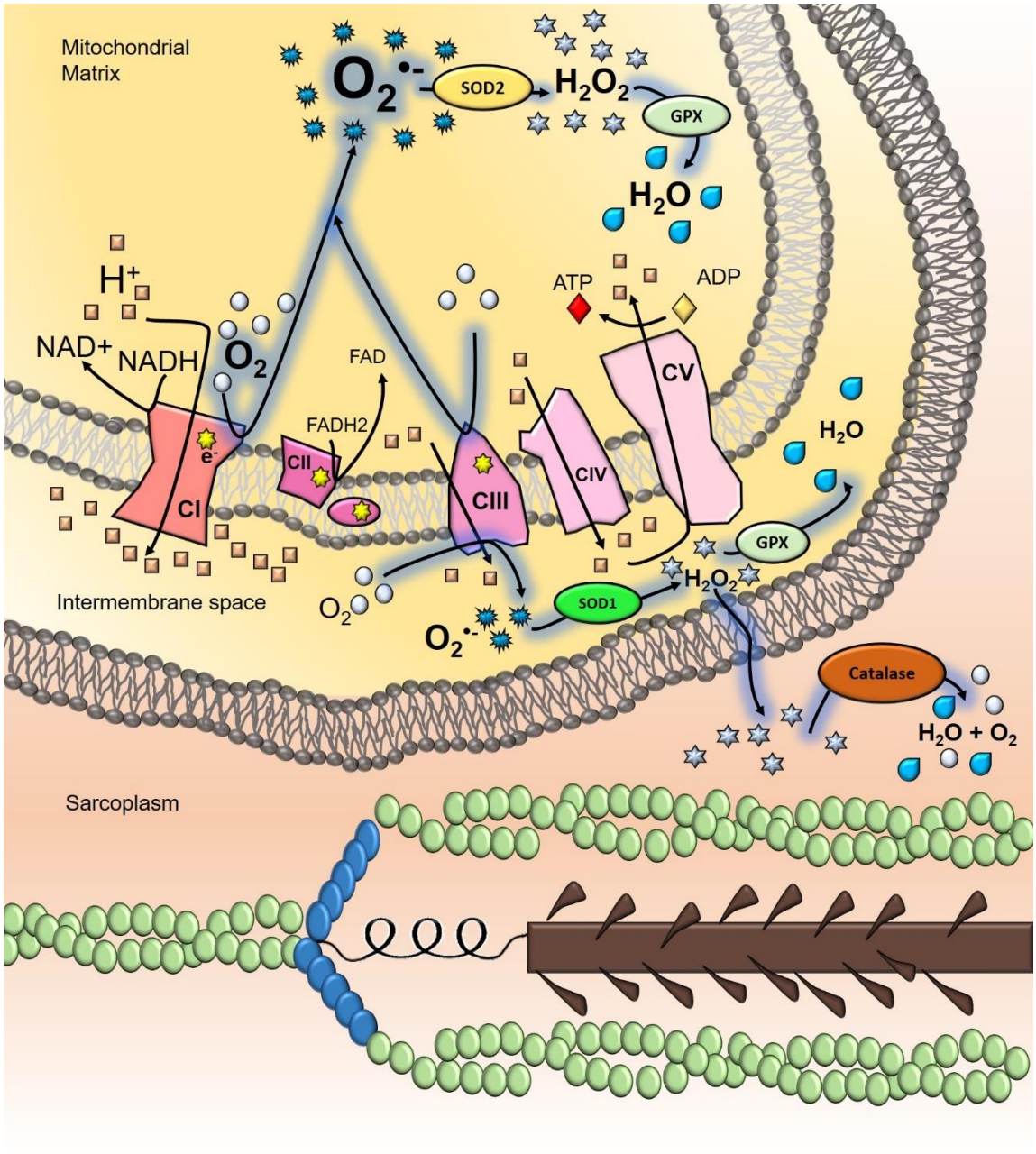

Figure 7. Illustration of mitochondrial ROS production and scavenging. Mitochondrial ROS is thought to be mainly produced by complex I and III (CI & CIII). Those can convert oxygen (O_2) to superoxide ($O_2^{\bullet-}$) either in the mitochondrial matrix or intermembrane space as illustrated above. Superoxide is scavenged by SOD1 in the intermembrane space and SOD2 in the mitochondrial matrix to hydrogen peroxide (H_2O_2). H_2O_2 is subsequently scavenged by GPX in the intermembrane space and mitochondrial matrix to water (H_2O), or by catalase (thought to be present in the peroxisomes) to H_2O and O_2.

1.5 COUNTERACTING MUSCLE WEAKNESS IN RA

The pathogenesis of RA is complex, and it is therefore difficult to find a marker to monitor the severity of the disease (15). Instead, the RA disease severity is measured through scoring systems that assess several factors such as the number of swollen and tender joints, the erythrocyte sedimentation rate, and a questionnaires that aim at measuring a patient's sensation of pain, fatigue, and overall health (15, 112). These scoring systems, e.g. the

commonly used disease activity score (DAS), can classify the state of RA in: remission, low disease activity, moderate disease activity and high disease activity (15). RA is currently treated through a so called “treat-to-target” approach. That means that the aim of the treatment of RA is disease remission which aims to improve the patient’s physical function, prevents the progression of joint damage, improves quality of life and ability to work and reduces comorbidity risks (15). The definitions of disease remission have been set in Europe and America, respectively, by the European League Against Rheumatoid Arthritis (EULAR) and American College of Rheumatology (ACR)(113, 114). Upon recommendation of EULAR, the current first line treatment of RA are short-term glucocorticoids and disease-modifying anti-rheumatic drugs (DMARDs) (113). DMARDs can be divided in conventional DMARDs (e.g. methotrexate and leflunomide) with a broad immunosuppressive activity and biological DMARDs (e.g. adalimumab and sarilumab) which target a specific proinflammatory protein such as TNF-α or IL-6 (15, 114). Current treatment options are efficient in retaining the patients in a state of low activity. However, despite better treatment options that keeps the disease in a state of low inflammation and low disease activity, patients with RA still suffer from deteriorated physical function, including muscle weakness. This indicates that muscle dysfunction is a complication that cannot be counteracted by anti-inflammatory medication alone.

2 AIMS

The overall aim of this thesis is to determine the role of oxidative stress in muscle weakness associated with rheumatoid arthritis. This is further divided into 4 specific sub-aims:

1. Elucidate muscle capacity (i.e. specific force production and intracellular Ca^{2+} handling) in skeletal muscles affected by arthritis and compare mouse models with patients with RA.

2. Define the role of peroxynitrite-induced oxidative stress on Ca^{2+} release, myofibrillar force and actin polymerization.

3. Identify intrinsic factors underlying decreased force production in skeletal muscle affected by arthritis.

4. Identify sources and scavengers of ROS that contribute to the altered ROS homeostasis in skeletal muscle afflicted by arthritis.

3 METHODOLOGY

3.1 ANIMAL MODEL AND HUMAN SUBJECTS

3.1.1 Study approval

All studies with animals were performed in accordance to the Swedish Animal Welfare Act, the Swedish Welfare ordinance and applicable regulations and recommendations from the Swedish authorities. The studies were approved by the Stockholm North Ethical Committee on Animal Experiments (see respective ethical numbers in the different papers). All studies with RA patients and healthy control persons were approved by the regional ethical review board in Stockholm (2014/ 516-31/2) and were all complied according to the Declaration of Helsinki. Both oral and written informed consent were given by the participants prior to participation in the study.

3.1.2 CFA induced arthritis

Induction of unilateral arthritis was done in C57BL/6JRj (Janvier) mice with Complete Freund's Adjuvant (CFA, Chondrex) in either the ankle (5uL at 10ug/ul) or knee joint (10uL at 10ug/ul). The mice were anesthetized with isoflurane prior (4% induction, 2.5% maintenance) to the intra-articular injection. The mice were monitored daily for their health and were housed at the local animal facility with a 12h light-dark cycle and food and water were provided *ad libitum*. The diameter of the knee and ankle joints were measured with a caliper every other day and the mice were sacrificed at the end of each experiment (either 24h or 2 weeks after induction of arthritis).

3.1.3 RA patients and healthy control persons

Eleven patients with RA and eleven healthy control persons participated in the study. All patients had seropositive RA according to criteria of the American College of Rheumatology, ACR 1987, and were on stable disease modifying anti-rheumatic drugs (DMARDs). Their disease activity was determined by calculation of the disease activity score (DAS). More detailed information of the RA patients can be found in Supplemental Table 4 of Paper I. The healthy control group was age-matched (45-62 years old) and were women without an inflammatory disease. All participants were subjected to a biopsy of their quadriceps vastus lateralis muscle, a Biodex force measurement of the force in their legs, a CT scan of their legs and activity measurement with an accelerometer.

3.2 MEASUREMENTS OF FORCE AND PHYSICAL ACTIVITIY

3.2.1 *Ex vivo* force measurements

Extensor digitorum longus (EDL) muscles were dissected from mice for *ex vivo* force measurements. Muscles were kept in a Tyrode solution (containing in mM: 121 NaCl, 5 KCl, 1.8 CaCl2, 0.4 NaH_2PO_4, 0.5 $MgCl_2$, 24 $NaHCO_3$, 0.1 EDTA and 5.5 glucose, gassed with 95% O_2/5% CO_2 to achieve a bath pH of 7.4). The muscles were subsequently tied with a silk knot around the tendon and placed in an organ bath to a force transducer and adjustable

holder (World Precision Instruments). Contractile force was measured at a range of frequencies (1-150Hz) through stimulating the muscles with supramaximal pulses after stretching the muscles to optimal muscle length L_0. Absolute force was calculated through conversion of mV to mN. Specific force was calculated by normalizing the absolute force with the CSA of the muscle, which was assessed by dividing the muscle mass by the product of muscle length and density (1.06 g/ cm^3).

3.2.2 Dissected single FDB fiber force measurements

Single flexor digitorum brevis (FDB) fibers were obtained by dissection and thereafter mounted in a chamber between a force transducer and an adjustable holder, as described in Paper I. Briefly, the fibers are constantly super-fused with Tyrode solution (containing in mM: 121 NaCl, 5 KCl, 1.8 CaCl2, 0.4 NaH_2PO_4, 0.5 $MgCl_2$, 24 $NaHCO_3$, 0.1 EDTA and 5.5 glucose, gassed with 95% O_2/5% CO_2 to achieve a bath pH of 7.4) and contractile force was measured at a range of frequencies (1-150Hz) through stimulating the fiber with supramaximal pulses at optimal fiber length. $[Ca^{2+}]_i$ was measured with Indo-1 (Thermo Fisher Scientific) and mean fluorescence of Indo-1 was measured at rest and during tetanic contractions. An intracellular established calibration curve was used to convert mean fluorescence to $[Ca^{2+}]_i$ (115).

3.2.3 Myofibrillar force measurements

Myofibrillar force measurements were performed for Paper I and II. In brief, myofibrils were isolated from rabbit psoas muscle as previously described (116-118) and resuspended in rigor buffer (containing in mM: 10 imidazole, 100 KCl, 2 $MgCl_2$, 1 EGTA, pH 7.2) or relaxing buffer (20 imidazole, 7.2 mM EGTA, 13.74M $CaCl_2$, 5.4 mM $MgCl_2$, 68.7mM KCl, 5.6 mM ATP, and 14.4 mM creatine phosphate, pH 7, pCa^{2+} 9). The myofibrils were then incubated in either SIN-1 (Cayman Chemicals) [10mM] 10min at 4 °C or $ONOO^-$ (Cayman Chemicals) [0.05-2mM] in 0.3M NaOH. The reaction with SIN-1 or $ONOO^-$ was terminated through exchanging the buffer with new rigor or relaxing buffer without SIN-1 or $ONOO^-$. The myofibrils were then mounted to a glass needle and an atomic force cantilever in an experimental chamber placed on an inverted microscope. The length of the myofibril sarcomere was adjusted to 2.8μm and contraction was induced by adding activation buffer (containing in mM: 20 imidazole, 7.2 EGTA, 7 CaCl2, 5.4 MgCl2, 52.3 KCl, 5.7 ATP, 14.4 creatine phosphate, pH 7, pCa^{2+} 4.5). The deflection of the cantilever was measured by measuring the deflection of the laser light that was shined upon the cantilever. Through the known stiffness of the cantilever, the deflection of the light could be translated to force in $kN/\mu m^2$.

3.2.4 Biodex force measurements

RA patients and healthy control persons were subjected to Biodex force measurements of the force in their legs. The subjects were carefully positioned in the chair of a Biodex System 4 Pro (Biodex Medical Systems Inc.) and were instructed to perform isolated measurements of quadriceps muscle force. The force measurements consisted of 3 repetitions of maximal

isometric contractions with the angle of the knee at 120°. The measured peak torque in Nm was converted to specific force in kN/m^2 by using the defined length of the cantilever in which the leg was fixed and the cross-sectional area of the muscle which was obtained through a CT-scan of the leg. ImageJ was used to specifically measure the CSA of the quadriceps at the intermediate of the femur bone.

3.2.5 Accelerometry

All RA patients and healthy control persons were subjected to measurement of their daily activity with an accelerometer (GT, ActiGraph). The accelerometer was worn for 7 consecutive days and the obtained data was analyzed with the Actilife software. All periods of >90 minutes of consecutive inactivity were classified as non-worn periods and were excluded from the analysis using the algorithm of Choi et al. (119). Thereafter, the total activity in minutes was divided by the validated wearing period. The degree of activity was categorized according to the validated categorization of Freedson et al. (120).

3.3 MOLECULAR BIOLOGY

3.3.1 Purification of SR extracts and single RyR1 channels

SR extracts were obtained from pooled gastrocnemius muscle from healthy C57BL/6JRj mice. The muscles were homogenized in homogenization buffer (containing in mM: 300 sucrose and 5 imidazole, pH 7.4). The homogenate was centrifuged (20min, 12000 x g, 4 °C) and the pellet was resuspended in homogenization buffer and subsequently centrifuged again (same time, speed and temperature). The new supernatant was centrifuged in an ultra-centrifuge (Beckman Optima MAX-XP ultra-centrifuge) at 4 °C for 2h at 43 000 x g. Thereafter, the newly formed pellet containing RyR1 enriched SR fractions was resuspended in homogenization buffer. The volume of all buffers was kept constant at 10 w/w volume of the initial pooled muscle mass. All buffer contained protease inhibitor (containing in mM: 0.001 leupeptin, 0.001 pepstatin, 1 benzamide and 0.7 PMSF) and phosphatase inhibitor (containing in mM: 2 Na3VO4; 5 NaF; 1 β-glycerophosphate).

3.3.2 Immunoblots

Muscle tissue was homogenized in homogenization buffer (containing in mM: 10 Tris-maleate, 100 KCl, 2 $MgCl_2$, 2 EGTA, 2 $Na_4P_2O_7$, 1 $NaVO_4$, 25 KF, and protease inhibitor (Roche, 1 tablet/50 ml), pH 7.4). The homogenate was centrifuged at 4 °C for 10 minutes at 1000 x g. The supernatant was collected, and the protein concentration was measured with a Bradford assay (Biorad). Equal amounts of protein were separated in a gel by electrophoreses and transferred onto a PDVF membrane (Immobilon-FL, Milipore). Membranes were subsequently incubated with a primary antibody and secondary infrared-labeled antibody (see respective papers for antibody details) and washed with tris-buffered saline (TBS-T) (containing in mM: 50 Trizma® base, 150 NaCl) + 0.5% Tween (Sigma-Aldrich) in between. Immunoreactive bands were read with the LI-COR Odyssey Infrared Imaging System and analysis of the intensity of the bands was done with Image J.

3.3.3 RNA isolation

RNA was isolated from 20mg of muscle tissue obtained from interosseous or gastrocnemius muscle. This was done by homogenization of the muscles in RLT buffer (Qiagen) with 1% β-mercaptoethanol (BME) in a bead shaker. The homogenate was incubated with trizol and chloroform and centrifuged (10min, 12 000 x g, 4 °C). The aqueous phase was collected and incubated with chloroform and centrifuged (10min, 12 000 x g, 4 °C), which was repeated twice. After that, the new aqueous phase was collected and set to precipitate with isopropanol (Sigma-Aldrich) for 30 minutes at -20 °C. Centrifugation (10min, 12 000 x g, 4 °C) resulted in a pellet containing RNA which was then washed twice with ethanol before drying and diluting it in nuclease-free water (Thermo Fisher Scientific). The RNA concentration was measured with a spectrophotometer (NanoDrop, Thermo Fisher Scientific) after treatment of the RNA with Turbo DNase (Thermo Fisher Scientific).

3.3.4 Reverse transcription

Reverse transcription with SuperScript IV Reverse Transcriptase (Thermo Fisher Scientific) was used to convert RNA to cDNA. Oligo(dt) 20 and 10mM dNTP mix (Thermo Fisher Scientific) were added to 600ng RNA, which was then incubated for 5 minutes at 65 °C. The reverse transcription reaction was thereafter initiated at 50 °C after adding SuperScript IV and 1xRT buffer, 5mM MgCl2, 10mM DTT and RNaseOUT (1L20 diluted) (Thermo Fisher Scientific). After 50 minutes, the reaction was terminated at 85 °C for 5 minutes and subsequently the newly formed cDNA was cooled at 4 °C.

3.3.5 RT-PCR

RT-PCR was performed with 1:20 diluted cDNA from the reverse transcription step. The reaction mix consisted of iTaq™ Universal SYBR® Green supermix (Biorad) added to the cDNA with respective primers of the genes of interest in a 384 well plate. A melt curve protocol was applied with a C1000 Touch™ Thermo Cycler (Biorad): 1 cycle 95°C 3 min; 40 cycles of 95 °C 10 seconds, 1 cycle 60 °C 30 seconds. SYBR® Green fluorescence was measured to determine the Cq values of the different genes of interest. RT-PCR data was analyzed by normalization towards housekeeping genes HPRT and Rplp0 by using the ΔΔCt method.

3.4 ACTIN POLYMERIZATION AND SINGLE CHANNEL RECORDINGS

3.4.1 Actin polymerization assay

Actin polymerization was measured using a pyrenyl-assay (121). G-actin (Cytoskeleton, AKL99) was solubilized in G-buffer (containing in mM: 5 Tris-HCl, 0.1 CaCl2, 0.5 ATP, 0.5 DTT, pH 7.6) and thereafter incubated in SIN-1 [5, 10 or 20mM], 15 min at room temperature. Actin concentration was determined by measuring absorbance using the excitation coefficient of actin E= 0.63 ml/ mg x cm as previously described (122). Actin [8 μM] and pyrene-labelled actin [4% of actin concentration] were added to a dark 96 well plate. EGTA and $MgCl_2$ [0.2 and 0.05mM respectively] were added to replace actin bound Ca^{2+} for

Mg^{2+}. Ten minutes later, polymerization of actin was induced, by addition of $MgCl_2$ and KCl [1 and 100mM respectively] and the polymerization was followed by excitation at 365 nm and emission detection at 410 nm (Fluoroskan II, Labsystems). The steady state fluorescence was measured 24h and 48h after induction of polymerization.

3.4.2 Single RyR1 channel recordings

Isolated single RyR1 channels from SR fractions, were added to a lipid bilayer that separated a cis (cytoplasmic) and a trans (luminal) solution (cis containing in mM: 230 Cesium Methanesulfonate (CsMS), 20 CsCl, 1 CaCl2, and 10 TES, pH 7.4; trans containing in mM: 30 CsMS, 20 CsCl, 1 CaCl2, and 10 TES, pH 7.4). The RyR1 channels were added to the cis solution so the cytoplasmic surface faced the cis solution after incorporation in the lipid bilayer. The [Cs^+] in the trans solution was raised to 250mM by addition of 200mM CsMS. To achieve a final free [Ca^{2+}], 2mM ATP and ~1.32mM 1,2-bis (o-109 aminophenoxy)ethane-N,N,N′,N′-tetraacetic acid (BAPTA) were added. Recordings of the open probability (P_o) of the channel were done by measuring the current flow through the channel at +40 and -40 mV at 23°C. These voltages ensured a large current flow through the channel. The data obtained was analyzed using the Channel 2 program (developed by P.W. Gage and M. Smith, John Curtin School of Medical Research, Canberra, Australia). All data was sampled at 5kHz, filtered at 1 kHz and the baseline noise was excluded which was set as ~20% of the maximum single-channel conductance measured as P_o.

3.5 ANALYTICAL ANALYSIS OF PROTEIN BIOLOGY

3.5.1 Mass spectrometry

With mass spectrometry the oxidative post-translational modification (oxPTMs) were identified on RyR1 and actin. Specifically on: (i) actin from myofibrils incubated in SIN-1, (ii) purified actin (Cytoskeleton AKL99) incubated in SIN-1, (iii) actin from skeletal muscle from mice with CFA-induced arthritis, (iv) actin from skeletal muscle from patients with RA and (v) RyR1 from SR-extracts incubated in SIN-1. The protein samples were digested with trypsin and subsequently cleaned in a HyperSep plate and dried in a speedvac centrifugal evaporator. The trypsin-digested peptides were separated by chromatography and ionized by electrospray in an Orbitrap QExactive Plus mass spectrometer (Thermo Fisher Scientific). The survey MS spectrum was acquired at a resolution of 60.000 (m/z range 200-2000). The MS/MS data were extracted with RawtoMGF software and analyzed with Mascot (Matrix Science, version 2.5.1) and X!Tandem (thegpm.org; version CYCLONE 2010.12.01.1). Variable post-translational modifications of amino acids were set as tyrosine nitrations, cysteine nitrosylations and MDA modifications alongside fixed modifications as cysteine carbamidomethylations that were introduced as a result of sample preparation. The protein prophet algorithm (123) was used to assign protein probabilities and Scaffold (version Scaffold_4.4.5, Proteome Software Inc.) was used to validate the identified MS/MS-based peptides and post-translational modifications.

3.5.2 Chimera 3D protein modeling

All validated variable post-translational modifications on actin and RyR1 were visualized in the 3-dimensional crystal structure of either actin or RyR1 (see the respective papers for the PDBe protein codes and references). Prior to visualization, ClustalW (124) was used to investigate the amino acid sequence homology between rabbit, human and mouse actin and between rabbit and mouse RyR1. The UCSF-Chimera software (ref 25 paper III) was used to find the location in the 3-dimensional model of actin or RyR1. The modifications were subsequently presented as spheres and annotated with their one-letter code specifier in the respective figures of paper I and III.

3.5.3 Molecular dynamic simulations

Molecular dynamic simulations were performed with Gromacs (simulation package 5.1.2.) (125) on the 3.3Å structure of rabbit skeletal muscle F-actin, PDBe 2ZWH, which includes all amino acid residues of actin and has previously been used in molecular dynamic-simulation studies (126-128).The F-actin structure was solvated in a truncated dodecahedron box for minimal distance between any protein atom and 52 K^+ and 39 Cl^- ions were added for neutralizing the protein and mimicking an ionic strength of 0.15M. A force field was applied (129) for all atoms except Ca^{2+}, K^+ and Cl^-. The LINCS (130) algorithm was used to constrain the length of bonds during the molecular dynamic runs. Other parameters were set such as temperature (300K), pressure (coupled to an external bath with the Parrinello-Rahman algorithm (131) and van der Waals forces (truncated at 1.0nm). The long-range electrostatic forces were treated using the particle mesh Ewald method (132, 133). Four molecular dynamic simulation replicates of each 100ns were performed and the analysis of those was performed with use of Gromacs.

3.6 MEASUREMENTS OF ROS SOURCES AND ROS SCAVENGERS

3.6.1 Electroporation of roGFP for live cell imaging of ROS

Reduction-oxidation sensitive genetically encoded green fluorescent protein (roGFP) plasmids targeted to the mitochondria (mito-ro1GFP) (134) or NOX2 (p47phox-roGFP2) (135) were amplified in *E. coli* bacterium at 37°C. The plasmid-DNA was purified after 24h with a maxi-prep E.Z.N.A.® kit (Omega Bio-tek) according to manufacturer's instructions. Hyaluronidase (10u, 2μg/μl) was injected in the footpads of the mice 1h prior to plasmid electroporation. The roGFP plasmids were injected in the footpad of C57BL/6JRj mice (Janvier). Electroporation in the flexor digitorum brevis muscle (FDB) happened through giving 20 electric pulses of 1Hz for 20ms at 100V to the plasmid-injected footpad of the mouse. After electroporation, the mice were injected with TEMGESIC (35 μl/ mL PBS) to reduce pain caused by the electroporation protocol.

3.6.2 Single muscle fiber dissociation

FDB muscles were dissected in Tyrode (containing in mM: 121 NaCl, 5 KCl, 1.8 $CaCl_2$, 0.4 NaH_2PO_4, 0.5 $MgCl_2$, 24 $NaHCO_3$, 0.1 EDTA, and 142 5.5 glucose) from mice with CFA-induced arthritis in the ankle, 24h or 2 weeks after induction of arthritis. The muscles were then

incubated in collagenase type I (3 mg/ml in DMEM+ 10% FBS) in an incubator (37°C, 5% CO_2) for 2h. Thereafter the dissociated muscles were gently pipetted to separate them and then transferred into fresh DMEM and cultured on 2% laminin-coated plates (MatTek) for roGFP live cell imaging or on a Nunc™ Lab-Tek™ chambered cover-glasses for immunofluorescence imaging of ROS scavengers.

3.6.3 RoGFP live cell imaging for ROS production

Live ROS production was measured in dissociated FDB fibers expressing mito-ro1GFP or p47phox-roGFP2 in muscle afflicted with inflammation (24h after induction of arthritis with CFA) or control muscle (injections were done as described above). A three steps protocol was followed whereby the mito-ro1GFP and p47phox-roGFp2 probes were excited at 488nm and emitted light was collected at >500 nm. In the first step the fibers were perfused with Tyrode (containing in mM: 121 NaCl, 5 KCl, 1.8 $CaCl_2$, 0.4 NaH_2PO_4, 0.5 $MgCl_2$, 24 $NaHCO_3$, 0.1 EDTA, and 142 5.5 glucose) in order to capture baseline fluorescent emitted light. Tyrode was then exchange for Tyrode with DTT (1mM) to reduce the cellular environment and thereby detect the maximum fluorescence (F_{max}). Last, Tyrode with DTT was exchanged for fresh Tyrode without DTT, to capture ROS production for a minimum of 20 minutes. All imaging was performed with a confocal imaging microscope (Zeiss LSM700, 40x zoom, water-based lens). The analysis of fluorescent intensity of each cycle was performed in ImageJ and normalized to F_{max}.

3.6.4 Immunofluorescent imaging of ROS scavengers

Dissociated FDB fibers were fixed with paraformaldehyde for 20 min at room temperature and subsequently washed with PBS and blocked for unspecific antibody binding with goat serum. Thereafter, the fibers were stained with primary antibodies for ROS scavengers SOD2 (Ab13533, Abcam), catalase (Ab16731, Abcam) and α-151 actinin (A7811, Sigma) and incubated with secondary antibodies (anti-153 rabbit A11035, anti-goat, A32816, anti-mouse, A11029, Thermofisher). Images were captured with a super-resolution Zeiss LSM800 Airyscan microscope (resolution: 2.997 pixels per micron; 40x zoom) and analyzed with ImageJ.

3.6.5 Catalase activity assay

The enzymatic activity of catalase was measured with a colorimetric assay (ab83464, Abcam) in homogenized interosseous muscle from mice with CFA-induced arthritis. The interosseous muscle from both the arthritic and control leg were homogenized in 20 weight/ volume catalase assay buffer. Protein concentration in each sample was measured with a Bradford (Biorad) assay. Equal amounts of protein were loaded in a 96-well plate and incubated with H_2O_2 for 30 minutes at 35 °C. The H_2O_2-sensitive dye OxiRed (Abcam) was added after the incubation period and the absorbance was measured at 570nm. The amount of H_2O_2 converted by catalase over time was calculated by means of a standard curve.

3.7 STATISTICS

The data of this thesis is analyzed through the following statistical approach. Mean data is presented ± SEM. For all statistical analysis, first the normal distribution was tested with a

Shapiro-Wilk and equal-variance was tested with a Brown-Forsythe test. If the data set contained no equal variances, then a Mann-Whitney test was used. A data set that passed the Shapiro-Wilk test ($P > 0.05$) and Brown-Forsythe test ($P > 0.05$), was compared using an unpaired two-tailed Student's t-test. Difference among more than 2 groups were analyzed with an ANOVA test with a Tukey's honest significant difference post hoc test, followed by a Bonferroni's multiple comparison test. Linear regression analysis was used to determine the degree of linear correlation between two seemingly linear dependent values. In all analysis, a P value less than 0.05 was considered significant (* $P < 0.05$; ** $P < 0.01$; *** $P<0.001$). The analysis was performed using Sigma plot 13.0 (Systat Software) or Prism 7 (GraphPad).

4 RESULTS AND DISCUSSION

4.1 OXIDATIVE MODIFICATIONS ON ACTIN PROMOTE MUSCLE WEAKNESS IN RA (PAPER I & II)

4.1.1 Decreased force of muscle from mice with arthritis

In order to understand how RA causes muscle weakness, we investigated the effects of arthritis on the skeletal muscle performances with taking in consideration the muscle size. Arthritis was induced by unilateral intra-articular injection of Complete Freund's adjuvant in the knee or ankle joint of C57BL/6JRj mice. At peak inflammation, i.e. 2 weeks after induction of arthritis, the diameter of the respective injected ankle or knee was significantly bigger than in healthy control mice (**paper I, suppl. fig. 1A &B**). At this time point, the muscle force was measured *ex vivo*, in both whole muscles and single muscle fibers of the arthritic leg and the healthy control leg. A significant decreased force was observed in both whole muscle and single muscle fibers affected by arthritis compared to healthy control (Ctrl) muscles (**paper I, fig. 1F & suppl. fig. 1C&D**). The cross-sectional area (CSA) of the EDL and FDB fibers was however not significantly different between healthy control muscles and muscles from the arthritis leg (**paper I, fig. 1 G & suppl. fig. 1E&F**). In contrast to other models of arthritis such as collagen-induced arthritis (CIA)(2), mice with CFA-induced arthritis develop an inflammation that is primarily localized to the local area of the injection. Indeed, unilateral induction of arthritis with CFA, did not affect the force in the muscles of the contralateral leg. The force production of these muscles was namely not significantly different from muscles from wild-type C57BL/6JRj mice (**paper I, suppl. fig. 1C**).

4.1.2 Altered Ca^{2+} handling of muscles from mice with arthritis

As described in the introduction, section 1.2.3., intrinsic muscle dysfunction can be an effect of altered Ca^{2+} handling (19). Ca^{2+} release from the SR through RyR1 is necessary to uncover the myosin binding sites on actin. Subsequently, Ca^{2+} enables actin-myosin cross bridge formation, hence a higher $[Ca^{2+}]_i$ results in increased myofibrillar force until saturation of $[Ca^{2+}]_i$ and saturation in the number of force generating actin-myosin cross bridges (31, 97). In mice with CFA-induced arthritis in the ankle, the tetanic $[Ca^{2+}]_i$ of the muscle fibers from the arthritic leg, did not significantly differ from the tetanic $[Ca^{2+}]_i$ in muscle fibers of the control leg at stimulation frequencies 1 till 150 Hz although a significantly declined force (**paper I, fig. 1H-I**). Moreover, the Ca_{50}, i.e. $[Ca^{2+}]_i$ at 50% of peak power (P_{max}), was neither significantly different between the muscle fibers affected by arthritis and the control muscle fibers. These results indicated that Ca^{2+} release and myofibrillar Ca^{2+} sensitivity was not affected by CFA-induced arthritis. To effectively release all Ca^{2+} stored in the SR, skeletal muscle fibers can be incubated with caffeine (5mM) and stimulated at high-stimulation frequency (120Hz) (71). Indeed, Ca^{2+} release was enhanced by caffeine at 120Hz stimulation in muscle fibers affected by CFA-induced arthritis and healthy control fibers yet did not significantly differ between the arthritis affected muscles and healthy control muscles and neither did it improve force production (**paper I, fig. 1J-K**). These results showed that the tetanic force at 120Hz of the healthy control muscle fibers after caffeine application was close to maximum. However, in the arthritis affected muscle fibers, the force did not improve to the

level of the control muscles, despite caffeine induced Ca^{2+} release that would enable maximum force production at 120Hz. These results suggest that in mice with CFA-induced arthritis, the lower force in muscles affected by arthritis is caused by a decreased ability of actin and myosin to generate myofibrillar force rather than the other two hypothesized causes of intrinsic muscle weakness, i.e. decreased Ca^{2+} release or decreased myofibrillar Ca^{2+} sensitivity.

4.1.3 Decreased force of muscles from patients with RA

Previous research of muscle strength in RA patients, e.g. by Ekdahl and Broman, have not normalized muscle force towards the muscle size (6). However, already in 1994 Helliwell and Jackson reported that only ~40% of the decreased muscle strength can be explained by a decrease in muscle size (12). It may be to notion that, in addition to measuring absolute force, measuring muscle force in RA patients and normalizing muscle force to muscle size, gives extra information how muscle weakness persists in RA patients. We have therefore assessed the physical capacity of RA patients through measurements of the force produced by the thigh muscles (quadriceps femoris) and normalized it to the size of the muscle which was measured by a CT-scan. The RA patients included in this study had a moderate state of the disease (average DAS of 3.3 ± 0.4) and all presented arthritis in the lower extremities (**paper I, suppl. table 4**). In addition, all patients were being treated with DMARDs that target pro-inflammatory signaling such as TNFα or a general immunosuppressant. In the RA patients of this study, the specific force, i.e. normalized to CSA, of quadriceps femoris was significantly lower than the specific force of age- and weight-matched healthy women (**paper I, fig. 5 B**). The CSA of the quadriceps muscle of the RA patients was not significantly different than the CSA of the quadriceps muscle of the healthy control subjects (**paper I, fig. 5D**). Thus, although the RA patients were on stable DMARD therapy, the results show that RA patients present muscle weakness which cannot be explained by altered muscle size, comparable to the observed results in rodent models of arthritis and the CFA mice of our study. Inflammation-induced pain may be a contributing factor to a sedentary behavior in RA patients and which could contribute to reduced muscle performance. We investigated if the decrease in force could be linked to a lower physical activity in RA patients than in healthy control persons. However, accelerometry measurements showed no difference in daily physical activity or degree of physical activity between the RA patients and the healthy control persons (**paper I, fig. 5D-E**). In fact, it is possible that the previous resistance for RA patients to perform physical activity have been associated with a lack of education and information about the benefits of physical activity and insufficient awareness among rheumatologists, rather than an increased perception of pain by the RA patient (136). Moreover, patients with increased physical activity have a decreased the perception of pain and fatigue (137). Altogether, this supports the observed results that muscle weakness in RA patients cannot solely be explained by a decrease in muscle mass or that physical inactivity contributes to the muscle weakness of the patients of our study.

Although the muscle mass did not appear to different in the RA patients compared to healthy control persons, the muscle quality may have changed without a change in muscle mass (e.g. increased muscle fibrosis). Muscle fibrosis is defined as excessive accumulation of extra cellular matrix components, especially collagens, in skeletal muscles (138). Thus, fibrosis may be a contributing factor to the observed decreased muscle strength in RA patients. However, it was not studied in detail in paper I, but should be paid attention in future studies. Nevertheless, the data from paper I and previous studies infer that an intrinsic muscle dysfunction contributes to muscle weakness in RA. Intrinsic muscle dysfunction is associated with oxidative stress not only in RA (2, 3, 19), but also in sepsis (8, 57, 117), muscle dystrophy (139, 140), malignant hyperthermia (45), aging (80), heart failure and stroke (141, 142), ventilatory-induced diaphragm dysfunction (143, 144) and cancer (7). As a matter of fact, in the mice with CFA-induced arthritis from this study, a significantly higher level of 3NT oxPTMs was observed on muscle proteins in the arthritis affected muscles compared to the control muscles (**paper I, fig. 1B-E**). Therefore, the functional effects of oxPTMs on myofibrillar force, actin polymerization and RyR1 gating were studied.

4.1.4 Declined myofibrillar force

The effects of oxPTMs on myofibrillar force were assessed with atomic force cantilever experiments. Oxidative 3NT modifications were introduced on myofibrils with $ONOO^-$ or with the $ONOO^-$ donor SIN-1. Myofibrillar force was significantly reduced in myofibrils that were incubated in $ONOO^-$ and SIN-1 compared to control conditions (**paper II, fig. 1 & 2**). DTT reduces cysteine nitrosylations that can be introduced by SIN-1. Myofibrils incubated in SIN-1 in the presence of DTT, also presented a significant reduction in force compared to control myofibrils (**paper I, fig. 2A-C**). These results thereby showed that $ONOO^-$-induced modifications on myofibrils, such as 3NT (**paper I, fig. 2D**), can have direct negative effects on muscle force production. The isometric myofibrillar force of a myofibril is dependent on the actin-myosin cross bridge kinetics (34). The relationship between isometric myofibrillar force an actin-myosin cross bridge kinetics can be described as follows:

$$F = n_{CB} F_{CB} \frac{f_{app}}{f_{app} + g_{app}}$$

Herein is, F the isometric force of a myofibril (i.e. myofibrillar force), n_{CB} the number of actin-myosin cross bridges, F_{CB} the force per cross bridge, f_{app} the rate of cross bridge attachment and g_{app} the rate of cross-bridge detachment (34). Furthermore:

$$\frac{f_{app}}{f_{app} + g_{app}} = \frac{k_{Tr} - k_{LIN}}{k_{Tr}}$$

The force (F) parameter can be measured with a regular myofibrillar force measurement. On the other hand, k_{Tr} can be measured with atomic force cantilevers during a so called "myofibrillar force redevelopment experiment". The rate of force redevelopment is k_{Tr}. In such an experiment, a myofibril is shortened with 15% of the initial myofibril length during

steady state activation at pCa 4.5. Then the myofibril is let to redevelop force until steady state, followed by relaxation of the fiber at pCa 9.0. The parameter k_{LIN} is the rate of slow (linear) relaxation of a myofibril. There are two phases of myofibrillar relaxation after decreasing free [Ca^{2+}]: (i) an initial slow relaxation phase where myofibrillar force declines while sarcomeres remain isometric and (ii) a fast relaxation phase where myofibrillar force declines while longitudinal movements within the sarcomere occur. In addition to F and k_{Tr}, k_{LIN} can also be measured with atomic force cantilevers. This is possible after deactivation of the myofibril by lowering free [Ca^{2+}] (**paper II, fig. 5B**). Myofibrillar force measurements in combination with a myofibrillar force redevelopment experiments can thus provide detailed information about how oxPTMs can affect actin-myosin cross bridge kinetics.

In myofibrils incubated with $ONOO^-$ or SIN-1, no change was observed in k_{Tr} (**paper II, fig. 3E**). On the other hand, k_{LIN} was significantly increased in myofibrils incubated in SIN-1 compared to control conditions (**paper II, fig. 6A**). Because k_{Tr} was not changed and k_{LIN} was increased in myofibrils carrying oxPTMs, the ratio $\frac{k_{Tr}-k_{LIN}}{k_{Tr}}$, and thus $\frac{f_{app}}{f_{app}+g_{app}}$, decreases compared to control myofibrils (**paper II, table I**). Moreover, the decrease in $\frac{f_{app}}{f_{app}+g_{app}}$ is of similar magnitude as the decrease in myofibrillar force (i.e. ~55%) (**paper II, table I**). These results suggest that a decreased myofibrillar force due to oxPTMs is likely attributed to an increase in k_{LIN}. The properties of k_{LIN} predominantly reflect a transition of actin-myosin cross bridges from a force generating state to a non-force generating state (144-146).

Together these results show that myofibrils carrying 3NT modifications produce less force which is likely caused by a decreased capacity of actin and myosin to form force generating cross-bridges.

4.1.5 Compromised actin polymerization

Actin forms the centrally located structure of the thin filaments of myofibrils. We investigated the effects of oxPTMs on actin polymerization by incubating G-actin with SIN-1 and measuring actin polymerization with an actin polymerization assay (**paper I, fig. 2**). Actin polymerization was initiated through increasing the [Mg^{2+}] (allowing for exchange of Ca^{2+} to Mg^{2+} bound to G-actin, which induces polymerization *in vitro*) under conditions with DTT. The polymerization rate was significantly lower for actin carrying oxPTMs introduced by SIN-1 than for unmodified actin (**paper I, fig. 2**). These results agree with previous observed finding from Clements et al. showing that the rate of actin polymerization declines after incubation of actin with the $ONOO^-$ donor SIN-1 (148). Moreover, we showed that the steady state polymerization level, measured 24h and 48h after initiation of polymerization, was significantly decreased by SIN-1. Altogether, this shows that G-actin carrying oxPTMs may thus still be able to form F-actin filaments however the oxPTMs compromise the stability of the F-actin filament. Moreover, F-actin filaments with G-actin monomers

carrying oxPTMs may be sterically hindered and hence cause an impaired ability of actin to bind with myosin and thereby impair myofibrillar force.

4.1.6 3NT and MDA modifications on actin

To further elucidate how oxPTMs on actin can cause decreased actin polymerization and decreased force production we used mass spectrometry to identify the modified amino-acid residues carrying an oxPTM for actin from myofibrils and monomeric G-actin incubated in SIN-1 (**paper I**). It is important to note that the amino acid sequence of skeletal muscle actin, (i.e. α-actin) is conserved in human, mouse and rabbit (**paper I, supplementary table 2**). This has made it possible to identify the location of all 23 modified amino acid residues of actin from SIN-1 incubated myofibrils (n=3) and monomeric G-actin (n=3) and compare them with those modified in weakened skeletal muscles of mice with CFA-induced arthritis (n=3) (**paper I, fig. 3B-D & suppl. table 1**), as well as the patients with RA. Two types of oxPTMs were identified on actin with mass spectrometry: 3NT and MDA. The location of the amino acids carrying a 3NT or MDA modification, were visualized in the crystal structure of ATP-bound α-actin (65) (**paper I, fig. 3**). Intriguingly, the modified amino acids of actin were at the exact same location or close to each other in the actin from mice with arthritis and the SIN-1 treated actin samples. Therefore, we have called these locations "hotspots" of oxidative modifications, as these regions of the conserved actin structure appeared to be specifically sensitive to oxidative stress (**paper I, fig. 4A-C).** The first hotspot was located in subdomain 1 (SD1) and carried oxidative modified H101/MDA, Q360/MDA and Y362/3NT (**paper I, fig. 4A**). The second hotspot of oxidative modifications was around the flexible D-loop of actin in SD2, containing H40/MDA, Q41/MDA and Y53/3NT (**paper I, fig. 4B**). The D-loop is known to change confirmation upon ATP hydrolysis and plays an important role in the interaction of actin with myosin (64, 70). In addition, the D-loop is involved in longitudinal interactions within the F-actin filament (26, 149). Moreover, residue Y53 has previously been shown susceptible to $ONOO^-$-induced modification(150) and phosphorylation of this residue can cause slower actin polymerization and impaired actin filament stability (151-153). These results indicate that oxPTMs of hotspot 2 play a critical role with regards to decreased myofibrillar force and actin polymerization. The third hotspot was in SD3 and the observed oxPTMs were Y294/3NT, N296/MDA and N297/MDA (**paper I, fig. 4C**). These residues were found modified consistently at the same location in actin from mice with arthritis and the SIN-1 modified actin samples which stresses the conserved nature of actin.

4.1.7 3NT and MDA modifications on actin from RA patients

To see if the previous results also apply for patients with RA, we isolated actin from skeletal muscle biopsies from RA patients and identified the oxidative modifications with mass spectrometry. Indeed, oxPTMs were found in the oxidative hotspots of actin from the quadriceps muscles of RA patients (n=3) (**paper I, fig. 5G-I**). More specifically, a total of 11 consistent oxPTMS were found in subdomain (SD) 1, 2, 3 and 4 (**paper I, fig. 5F**) (SD1: H87/MDA, H101/MDA, and Q360/MDA; in SD2: H40/MDA, Q41/MDA, and Q59/MDA;

in SD3: H275/MDA, Y294/3NT, and N297/MDA; and in SD4: Y218/3NT and Q246/MDA). Molecular dynamic simulations were performed on the structural details of F-actin with particular regards to the identified oxPTMs in actin from patients with RA. This was done to investigate if the oxPTMs of the 3 hotspots in actin are indeed important for actin-myosin cross bridge formation and intra-actin filament connections. We looked at the root mean square fluctuations (RMSF), the solvent-accessible surface area (SASA), the number of H-bonds and the number of contacts of the oxPTMs. The root mean square fluctuations (RMSF) were assessed to study the flexibility of the different subdomains of actin. The highest flexible regions were found around MDA modified residues H40 and Q41 of hotspot 2 in SD2 of actin (**paper I, fig. 6a**). In this part of actin, the D-loop is located (residues 38-53). This region of actin also had the highest solvent accessibility, SASA (**paper I, fig. 6b**). Introduction of oxPTMs is a non-enzymatic mechanism and there is currently no consensus about the selectivity of the reaction. However, it is thought that the presence of nearby charged amino acids, i.e. Arginine (R), Lysine (K), Aspartic Acid (D), Glutamic Acid (E) or Histidine (H), provides a favorable environment for the introduction of oxPTMs (154-156). Indeed, in oxidative modified actin, the observed modifications of the residues in all the oxidative hotspots were located near charged amino acids (**paper I, suppl. fig. 3**). Moreover, due to the short half-life of ROS such as $ONOO^-$, ~5-20 ms and $O_2^{-\bullet}$, ~1 μs, the amino acids of actin that are susceptible to oxPTMs need to be close and accessible to the site of ROS (154, 157), and a high SASA could indeed allow this to be the case. In addition, also Q360 of hotspot 1 had a solvent accessibility similar to that of H40 and Q41 (**paper I, fig. 6b**). Q360 is located at the outer surface of the actin filament where addition of a covalently bound MDA adduct is likely to impose contacts of actin with other proteins. The modifications in hotspot 3, i.e. Y294/3NT and N297/MDA, were, intriguingly, located in regions with low flexibility and low solvent accessibility. We are unaware how these residues could have been accessible for modifications but Radi et. al. imply that local changes in the microenvironment can enhance the capacity of the residues to become modified independent of SASA, but the molecular details are unclear (43). Nevertheless, Y294 and N297 are proximal to a tight electrostatic network of the D-loop in the adjacent subdomain formed by H173, D286 and E270 (68). Modifications of Y294 and N297 may therefore result in disruption of the longitudinal intramolecular interactions of F-actin and can thereby cause instable F-actin filaments. Indeed, Y294 and N297 were those residues that were observed with the highest number contacts between non-hydrogen atoms separated by less than 4Å. In fact, all residues found modified in the 3 different hotspots had between 35 and 95 contacts (**paper I, fig. 6e**).

The results of the molecular dynamic simulations confirm that the modified residues in the hotspots in actin are residues important for actin filament stability and myosin interaction. Intriguingly, these hotspots were identified in all our experimental settings, i.e. in actin from weakened skeletal muscle from mice with arthritis, patients with RA, actin monomers with impaired polymerization abilities and weakened myofibrils with oxPTMs. The results together, show that oxPTMs in the oxidative hotspots of actin contributes to muscle weakness in mice with arthritis and patients with RA.

4.2 OXIDATIVE MODIFICATIONS INCREASE THE OPEN PROBABILITY OF RYR1 WHICH IS ASSOCIATED WITH RA-INDUCED MUSCLE WEAKNESS (PAPER III)

4.2.1 Increased RyR1 open probability

RyR1-mediated Ca^{2+} release from the SR is a tightly controlled process which enables muscle contraction (3, 25). Post-translational modifications can affect the function of the RyR1 complex. The RyR1 complex is known to be sensitive to redox modifications such as nitrosylation (88, 89), carbonylation (DNP) (45), MDA adducts (158, 159) and 3NT modifications (2). Well-studied post-translation modifications on RyR1 that activate the channel, are nitrosylation of cysteine residue 3635 (Cys3635) and phosphorylation of serine 2843 of RyR1 (S2843) (73). Altered RyR1 activity by redox modifications is known to contribute to hyperthermia crisis in environmental heat stress and malignant hyperthermia (160) and is associated with muscle weakness in dystrophy (140), aging (80) and breast cancer (7). In mice with arthritis, increased levels of 3NT modifications have been found on the RyR1-DHPR super-complex which were associated with altered Ca^{2+} release and muscle weakness (2). We investigated if introducing 3NT modifications with the $ONOO^-$ donor SIN-1, would affect the open probability of RyR1 channels (**paper III**). SIN-1 significantly increased the level of 3NT modifications on RyR1 (**paper III, fig. 1A**). The open probability (P_o) of RyR1 incubated in SIN-1, was significantly higher (3-fold) than the control condition (vehicle) (**paper III, fig. 1A&B**). SIN-1 is donating NO and $O_2^{-\bullet}$ to produce ONOO-, hence it can also lead to nitrosylation of RyR1 (56). To diminish the effect of cysteine nitrosylations, P_o was also measured of RyR1 incubated in SIN-1 in the presence of DTT. RyR1 incubated in SIN-1 with DTT had a lower open probability than RyR1 incubated in SIN-1 without DTT, however P_o was still significantly higher than the control conditions (**paper III, fig. 1C-D**). The effect of SIN-1 on RyR1 P_o was dose dependent, where P_o increased by ~30% with increasing SIN-1 concentration (0.2mM vs. 1mM SIN-1) (**paper III, fig. 1E**). Since the activity of RyR1 is depended on $[Ca^{2+}]$ (enhanced activation by low $[Ca^{2+}]_{cyt}$, i.e. nM compared to µM, (161, 162)), we also investigated if the effect of SIN-1 on the P_o of RyR1 was dependent on $[Ca^{2+}]$. However, there appears to be a weak, if any, Ca^{2+} dependence as SIN-1 increased P_o to a similar extent at 1nM and 100nM $[Ca^{2+}]$ (**paper III, fig. 1F**).

4.2.2 3NT and MDA modifications on RyR1

Several studies have shown that PTMs on RyR1 are associated with increased channel P_o, FKBP12 dissociation and SR Ca^{2+} leak (7, 29, 83, 84, 140). PTMs on RyR1 are often studied by immunoblotting with antibodies that detect the total amount of PTMs. On the other hand, mass spectrometry can detect the exact amino acids that are modified. The importance of identifying the exact modified residues becomes clear from studies that show that specific amino acid residues modifications of RyR1 are leading to altered gating properties of RyR1, i.e. Cys3635(88) and Ser2843(90, 92).

During sample preparation for mass spectrometry, DTT was used to reduce any cysteine nitrosylations introduced by SIN-1. A total of thirty oxPTMs were found on RyR1 incubated with SIN-1, being either 3NT (NO_2; +46 Da) or MDA-adducts (C_3H_3O; +54 Da) on basic amino acids (**paper III, fig. 2A**). Of those thirty, the location of 16 residues could be identified in the cytosolic shell and 8 in the core of the 3-dimensional crystal structure of RyR1 (PDBe: 5T15(74)) (**paper III, fig. 2A-C**). One RyR1 monomer consists of 5035 amino acid residues and there is currently no consensus regarding the selectivity of oxidative modifications. However, as mentioned the presence of nearby charged amino acids, provide supposedly a favorable environment for the introduction of oxPTMs (154-156). This agrees with the observed result that 23 out of 30 modifications were indeed flanked by charged amino acids (**paper III, suppl. table 1**).

In RyR1 incubated in SIN-1, the cytosolic shell contained two modifications in the N-terminal domain (NTD), i.e. N84/MDA and H379/MDA (**paper III, fig. 3B**). The NTD of RyR1 plays an important role in domain-domain interaction and multiple genetic mutations in NTD have been identified that underlie malignant hyperthermia, central core disease and multi-minicore disease (163). Interestingly H379/MDA is closely located to H383 which is a well-known disease mutation site (163).

A second cluster of modifications in the cytosolic shell, was found in the RyR repeat domains 1&2 (RY1&2) (**paper III, fig. 3C**): Y893/3NT, Y920/3NT, Q981/MDA and N991/MDA. In addition to RY1&2, oxPTMs were also found in the RY3&4 domain (**paper III, fig. 3D**): Y2855/3NT, Y2908/3NT, Q2931/MDA and Y2935/3NT. The four RyR repeats interact within the 3-dimensional structure, RY1&2 from one RyR1 monomer interacts with RY3&4 of the adjacent RyR1 monomer (**paper III, suppl. fig.1**). The modifications found in these domains may therefore disturb the intra-protein integrity. The RY3&4 domain is also referred to as phosphorylation domain and is a known site of phosphorylation which enhances the activity of RyR1(73). Ser2843 and Ser2814 of RY3&4 are well-studied residues that can get phosphorylated by PKA and CaMKII, respectively (73), and close to these and in the same domain we found oxPTMs Y2849/3NT (**paper III, table 1**) and Y2855/3NT (**paper III, fig. 3D**).

The spIA kinase and RyR (SPRY) domains of RyR1 mediate protein-protein interactions. The residues 671-681 of SPRY1 are involved in the binding of FKBP12 (73, 77). However, the exact residues that interact with FKBP12 are not yet fully elucidated and additional residues and even domains may also play a role in FKBP12's affinity to RyR1. In SPRY1 we found oxPTM Y808/3NT. SPRY2&3, comprising residues 1055-1656, contains the divergent region two (DR2) (residues 1298-1431(73)). The DR2 region plays an essential role in ECC. Deletion or substitution of the amino acids in the DR2 region has led to an inability to propagate ECC (73, 164). It is exactly in this region, we identified oxPTMs Y1332/3NT and Q1401/MDA (**paper III fig. 2A & table 1**).

RyR1 activity is inhibited by CaM at high $[Ca^{2+}]_{cyt}$ (161). CaM binds at three proposed binding domains (CaMBD) of the receptor (**paper III, fig. 4A**): CaMBD1 within residues

1975-1999 in the Junctional Solenoid (JSol), CaMBD2 within residues 3614-3640 in the BSol & Shell-Core linker peptide (SCLP) and CaMBD3 within residues 4295-4325, adjacent to the transmembrane helices(73, 165). The crystal structure of these domains has not yet been fully elucidated. However, it is clear that in RyR1 incubated in SIN-1, Q2017/MDA and Y2128/3NT of the JSol (**paper III, fig. 3G)** are close to CaMBD1 **(paper III, fig. 4B-C**).

RyR1 belongs to the group of the six-transmembrane (6-TM) ion channels (73). The core, or also called transmembrane part, has 6 helices that span the plasma membrane of the sarcoplasmic reticulum (S1-S6). In comparison to receptors of the group, e.g. transient-receptor potential (TRP) channels and voltage-gated potassium channels, RyR1 has an extraordinarily large cytosolic shell compared to the core (73, 74, 77). The voltage sensing domain is crucial for the voltage sensing function in other receptors of the 6-TM group and plays therefore an essential role in channel gating. However, in RyR1 the voltage sensing domain is not positively charged and therefore this domain has no voltage sensing function. Instead, the thus called pseudo voltage domain of RyR1 (also VSD-like domain), is thought to allosterically couple through mechanical conformational changes and thereby plays a role in RyR1 gating (73). It is in this domain, we found Y4687 and Y4554 modified with a 3NT modification close to the transmembrane helices (**paper III, fig. 5E**). Moreover, Y4554/3NT is closely located to CaMBD3 (**paper III, fig. 4C**). SIN-1 also induced oxPTMs in the core, in the SLCP domain (N3651/MDA, Y3657/3NT), the Core Solenoid (Y3765/3NT, Q3781/MDA) and in the Thumb and Forefinger (TaF) domain (Y4194/3NT) (**paper III, fig. 5B-E**). Thus, now we have identified where the modifications are and that they alter channel gating. For future studies would site-directed mutagenesis in combination with single channel recordings and cryo-EM be powerful tools to further elucidate how these oxPTMs affect the RyR1 function.

4.2.3 FKBP12 dissociation

The 12kDa protein FKBP12 binds to RyR1 and stabilize the channel. Removal of FKBP12 results in an increased open probability of the receptor (166). The RyR1 domains SPRY1 together with NTD, SPRY2&3 and JSol are thought to form a cleft for FKBP12 binding which binds with a stoichiometry of four FKBP12 proteins per RyR1 homotetramer (77, 78, 166). Oxidative stress on RyR1 has been associated with FKBP12 dissociation (7, 140, 158) and our mass spectrometry analysis on RyR1 incubated in SIN-1, identified oxPTM N84/MDA (NTD), H379/MDA (NTD), 249 Y808/3NT (SPRY1), Y1081/3NT (SPRY2&3), H1254/MDA (SPRY2&3), Q2107/MDA 250 (JSol) and Y2128/3NT (JSol) which were localized to the FKBP12 binding region (**paper III, fig. 6B-C**). As proof-of-concept, these modifications resulted in reduced FKBP12 bound to RyR1 with up to ~50% less FKBP12 bound to RyR1 after SIN-1 treatment as shown by immunoblotting experiments (**paper III, fig. 6D-E**).

4.2.4 3NT and MDA modifications on RyR1 from muscle affected by arthritis

Our results show that 3NT and MDA modifications are directly linked to increased RyR1 open probability and that oxPTMs are introduced in specific regions that could interfere with the gating of the channel. Increased RyR1 open probability, FKBP12 dissociation and Ca^{2+} leak are associated with reduced SR Ca^{2+} load and reduced SR Ca^{2+} release during ECC which could ultimately lead to impaired muscle contractility (7, 29, 83, 84, 140). Based on that oxidative stress on RyR1 is linked to the pathological process of many diseases, including RA (19) and cancer (7), and since higher levels of 3NT oxPTMs have been observed on the RyR1-DHPR super-complex in association with arthritis (2), we aimed at identifying oxPTMs on RyR1 from skeletal muscle affected by CFA-induced arthritis. However, we have so far not been able to identify 3NT and MDA oxPTMs on RyR1 from the arthritis affected muscles. In fact, that was almost expected since we had previously concluded that muscle weakness in mice with CFA-induced arthritis is caused by a myofibrillar problem (section 4.1.1 & 4.1.2) rather than a Ca^{2+} release complication. However, based on that stress associated PTMs on RyR1 (and RyR2 in cardiac) have most often been observed in more severe conditions (e.g. breast cancer-derived bone metastases(7), ventilator-induced muscle weakness (167) and heart failure (168), hence we believe that oxPTMs on RyR1 and altered Ca^{2+} release will appear in a later, more severe, stage of muscle weakness associated with RA (and here CFA). Nevertheless, the results from this study provide important information for continued efforts to understand RyR1 gating and the role of oxidative stress on RyR1 in pathophysiological conditions where oxidative stress and intrinsic muscle weakness play a role.

4.3 SOURCES AND SCAVENGERS OF ROS IN SKELETAL MUSCLES AFFECTED BY ARTHRITIS (PAPER IV)

Oxidative stress can be caused by an imbalance between the synthesis and scavenging of ROS (2, 3, 19, 36). Since we have shown that oxidative stress associated with RA promotes muscle weakness through introduction of oxPTMs on actin, we hypothesized that the balance between ROS sources and ROS scavengers is altered in muscles affected by arthritis. To test this hypothesis, we aimed to characterize the intramuscular pathways that underly oxidative stress in arthritis and contribute to muscle dysfunction. To that purpose we have looked at well-known sources of ROS and their respective scavengers in skeletal muscles of mice with CFA-induced arthritis (**paper IV**).

4.3.1 Decreased expression of mitochondrial complexes

Mitochondria can produce $O_2^{\bullet-}$ and H_2O_2 in skeletal muscle (37, 97). More precise, the mitochondrial complexes of the electron transport chain (ETC) can transfer electrons from their prosthetic group to O_2 which causes the formation of $O_2^{\bullet-}$ (96). Therefore, the protein and gene expression were investigated of the mitochondrial complexes in mouse skeletal muscle affected by arthritis (**paper IV, fig. 1**). As previously, arthritis was evoked in mice by unilateral injection of CFA in the ankle joint and mice were sacrificed after two weeks. At this time point, a drastic decrease in gene expression was observed for nuclear-encoded genes of the mitochondrial

complexes (I until IV) in the muscles of the arthritic leg compared to the healthy control leg (**paper IV, fig. 1B**). Simultaneously, the protein expression of complex I, II, IV and V was significantly decreased in the muscles affected by arthritis compared to the control muscles (**paper IV, fig. 1C-D**). The decrease in protein and gene expression of the mitochondrial complexes is indicative of a decreased oxidative phosphorylation capacity in muscles afflicted with arthritis.

4.3.2 Increased expression of scavengers SOD2, catalase and GPX1

$O_2^{\bullet-}$ is, under normal circumstances, rapidly scavenged to H_2O_2 by SOD2 and subsequently converted to H_2O and O_2 by catalase and GPX1 (37). The gene and protein expression of SOD2, catalase and GPX1 were therefore analyzed in skeletal muscles affected by arthritis (CFA-induced arthritis in the ankle) and compared with healthy control muscles. At the two-week time point, the protein expression of all three scavengers was significantly increased in muscle affected by arthritis compared to healthy control muscles (**paper IV, fig. 1E-F**). The gene expression of GPX1 was increased and that of SOD2 unchanged in the arthritis affected muscles (**paper IV, suppl. fig. 1**). At the same time, the gene expression of catalase was significantly lower in the arthritis-afflicted muscles. To check if the increased protein expression while decreased gene expression of catalase could resemble accumulation of inactive catalase, we also analyzed the catalase activity in both groups. However, the catalase activity was significantly higher in arthritis affected muscles than in healthy control muscles (**paper IV, fig. 1G**).

4.3.3 Altered subcellular location of ROS scavenger in muscles affected by arthritis

The previously described results suggest a higher ROS scavenging capacity in muscles afflicted with arthritis. The scavenging of $O_2^{\bullet-}$ and H_2O_2 is dependent on the subcellular localization of ROS scavengers, as ROS interact with protein and cellular targets in their immediate proximity (157). Here we used immunofluorescent staining and super-resolution imaging in skeletal muscle fibers to determine the subcellular localization of the ROS scavengers SOD2 and catalase in skeletal muscle fibers from mice with CFA-induced arthritis and healthy controls. The location of the scavengers was compared relative to α-actinin, an anchoring protein in the z-line of the sarcomere which is responsible for mechanical integrity (169).

SOD2 is a mitochondrial specific ROS scavenger (37) and electron microscopy from the striated skeletal muscle have shown that mitochondria are located at the z-line (170, 171). Indeed, in mice with CFA-induced arthritis, SOD2 expression could be observed at the Z-line in both muscle fibers affected by arthritis and healthy control muscle (**paper IV, fig. 2A&B**). On the other hand, SOD2 was also found expressed at the M-line at the center of the sarcomere in both arthritis affected muscle fibers and healthy control fibers. Whereas SOD2 expression was generally increased, the distribution of SOD2 expression at either the Z or M-line was not significantly affected by arthritis (**paper IV, fig. 2C-E**).

Catalase was found expressed at the z-line of the sarcomere, adjacent to the z-line (z') and at the M-line in both muscle fibers affected by arthritis and healthy controls (**paper IV, fig.**

3A). The location of the z' expression of catalase is ~150nm from the z-line, likely corresponding to the position of the peroxisomes. In contrast to SOD2, the distribution of catalase was significantly different in the arthritis-affected muscle fibers compared to healthy control fibers. The catalase expression was namely more pronounced at the z'-line in muscle fibers from the arthritic leg compared to muscle fibers of the control leg (**paper IV, fig. 3C-E**). The distance between peak catalase fluorescent intensity between Z and z'-line was therefore significantly reduced in the arthritis affected muscle fibers compared to healthy control fibers.

The significant increase of SOD2 and catalase expression and decrease in expression of mitochondrial complexes, suggest an enhanced ROS scavenging capacity in skeletal muscle affected by arthritis. An increase of catalase at a subcellular location that is close to the mitochondria, would imply enhanced scavenging of H_2O_2 to H_2O and O_2.

4.3.4 No increase of ROS production from mitochondria or NOX2

To investigate the subcellular ROS production in muscles affected by arthritis, ROS production from both mitochondria and NOX2 were assessed with redox sensitive ROS probes (roGFP). roGFP probes have two advantages: firstly, they are genetically encoded towards a specific site of ROS production such as the mitochondria (mito-roGFP) or NOX2 (p47phox-roGFP) (172). Secondly, roGFP probes are reversible: upon oxidation of their chromophore, mito-roGFP and p47phox-roGFP lose their excitability at 488nm which is reversible by reduction by for example DTT (172, 173). These probes thereby allowed us to follow ROS formation by the mitochondria and NOX2 in muscle fibers affected by arthritis in a three step protocol: first the baseline oxidation level in physiological Tyrode solution was established (i baseline), secondly the maximal fluorescence for each fiber was established with DTT (ii, DTT) and last the rate of oxidation was measured by quantifying the quenching of the roGFP probe over time after substituting Tyrode with DTT for fresh Tyrode (iii, post-DTT) (**paper IV, fig. 4A & 5A**).

Mito-roGFP or p47phox-roGFP were transfected into the FDB muscle of mice one week prior to induction of arthritis with CFA in the ankle. The ROS production was measured in isolated FDB fibers of both the arthritic leg and control leg, 24h after the induction of arthritis, to measure ROS production at an early active phase of the inflammation. The baseline oxidation level of mito-roGFP was not significantly different between muscle fibers affected with arthritis compared to healthy control fibers (**paper IV, fig. 4B**). After fully reducing the fibers with DTT, the rate of mito-roGFP oxidation and thereby mitochondrial ROS production was significantly lower in muscle fibers from the arthritic leg compared to muscle fibers of the healthy control leg (**paper IV, fig. 4C-E**). The increased expression of SOD2 and catalase in the arthritis affected fibers would support the observed decreased rate of mitochondrial ROS formation in muscle fibers of the arthritic leg compared to fibers of the control leg of mice with CFA-induced arthritis. SOD2 has a fast rate constant for scavenging $O_2^{\bullet-}$ to H_2O_2 (i.e. $2.3x10^9$ M^{-1} s^{-1}) (174). The rate of mitochondrial $O_2^{\bullet-}$ production depends on the concentration of enzyme responsible for transfer of electrons to O_2, the proportion of this

enzyme in a redox form that can react with O_2, and the second-order rate constant for the reaction of the enzyme with O_2 (96, 175). Mitochondrial complexes I and III are thought to facility the electron transfer to O_2 for the formation of $O_2^{\bullet-}$ in the mitochondria (37, 96, 175). This means that if the scavenging of mitochondrial produced $O_2^{\bullet-}$ is enhanced, shown by the increased SOD2 expression in arthritis affected fibers, and the mitochondrial complex expression is decreased, then the net $O_2^{\bullet-}$ production by the mitochondria in a balanced *in-vitro* environment may indeed be lower in arthritis affected muscles. Alternatively, the increased SOD2 and catalase expression and activity remove the $O_2^{\bullet-}$ and H_2O_2 at a faster rate than can be detected with the mito-roGFP probe. This knowledge in combination with the observed increase in catalase activity and expression at subcellular locations close mitochondria, supports the observed decreased rate of mitochondrial ROS production in arthritis affected fibers.

The ROS production from NOX2 was also significantly lower in arthritis affected muscle fibers compared to healthy control fibers. At baseline, the p47phox-roGFP fluorescence was significantly higher in the arthritis affected muscle fibers than in the healthy control fibers, showing that the probe was more reduced (**paper IV, fig. 5A-B**). The rate of ROS production by NOX2, after fully reducing the fiber with DTT, was significantly lower in arthritis affected fibers than in control fibers (**paper IV, fig. 5C-E**). In fact, the rate of ROS production by NOX2 in muscle fibers of the arthritic leg, was near zero. NOX2 is located in the sarcolemma and t-tubuli of the muscle and produces $O_2^{\bullet-}$ extracellularly which is converted by SOD to H_2O_2 (176, 177). This H_2O_2 can cross the membrane to exert intracellular effects and can be scavenged by catalase (37, 96). The expression of NOX2 has previously been found increased in muscles from rats with adjuvant arthritis (AIA)(3). However, here no significant difference could be found in NOX2 protein expression between arthritis affected muscle fibers and healthy control fibers (**paper IV, suppl. fig. 2A&B**).

Altogether, the results indicate that two of the primary considered sources of ROS production in skeletal muscle, are not the primary source of oxidative stress in the arthritis afflicted muscles of these mice. A result that is discussed further in the next section.

4.3.5 Treatment of mice with arthritis with the SOD2/ catalase-mimetic EUK-134 restores muscle force

The mito-roGFP and p47-roGFP measurements of the rate of ROS production, indicate that the primary cause of oxidative-stress induced muscle weakness associated with arthritis is not the result of a net increased ROS production by the mitochondria or NOX2. However, treatment (2 weeks, once daily from the start of the induction of arthritis) of mice with CFA-induced arthritis with EUK-134, a SOD/ catalase mimetic, counteracted muscle weakness (**paper IV, fig. 6**). In fact, it restored muscle force of the muscles afflicted with arthritis to levels similar of that of the control leg. These results are in agreement with earlier studies that showed that EUK-134 significantly improves skeletal muscle force in rats afflicted with a chronic inflammation (3, 178).

4.3.6 The sources and scavengers of ROS in skeletal muscles affected by RA: further studies are needed

Altogether the results of paper IV provide data that we currently cannot fully explain. We and others have repeatedly shown that oxidative stress is present in serum (38, 39) and skeletal muscle (2, 3) affected by arthritis. Moreover, we have shown that oxidative stress can result in muscle weakness. However, in paper IV, we observed an enhanced ROS scavenging capacity and reduced ROS production in muscle fibers afflicted with arthritis. Nevertheless, treatment with an antioxidant that mimics SOD2/catalase was capable to counteract arthritis-induced muscle weakness and we are currently investigating the oxidative stress levels in those muscles. However, two plausible explanations for our experimental results could be that in arthritis-afflicted muscles of CFA-mice (i.) the ROS production is increased but scavenged faster than the detection rate of the roGFP probes and/or (ii.) the source of ROS is different than mitochondria and NOX2 and close to that specific, yet unknown, site the ROS scavenging capacity is insufficient which results in oxidative stress and muscle weakness.

Furthermore, thus far only the ROS production rate from mitochondria and NOX2 have been investigated, other examples of ROS sources are NOS and PLA2 as described in section 1.4.2. Since EUK-134 is injected intra-peritoneally in mice with CFA-induced arthritis of this study, it is disseminated throughout the whole body of the mouse. It may therefore reach other sites of ROS production in the muscles where SOD2 or catalase are not efficiently neutralizing ROS, but we have so far no data to back up this hypothesis.

We measured the ROS production at 24h after the induction of arthritis. Nathan *et al.* (36) carefully described the term oxidative stress: an imbalance in the production and scavenging of ROS which will, when at the wrong place, for too long and too high levels, lead to e.g. irreversibly impaired cellular function and/ or pathological gain of function. Hence the time dependency of oxidative stress needs to be studied further in muscles that are affected by arthritis.

It is of importance to note that the rate of ROS production was measured in a balanced *in vitro* system. As mentioned in section 1.4.1, when the concentration of NADH increases, FMN of mitochondrial complex I can get more reduced whereby the production of $O_2^{\bullet -}$ increases. An increase of NADHP is hypothesized to happen in case of decreased respiration, ischemia or low ATP demand as a consequence of low respiration (96). Measuring mitochondrial oxygen consumption rate with an Agilent Seahorse experiment and stressing mitochondria with FCCP may therefore provide a better understanding of how mitochondrial ROS production is affected in muscles affected by arthritis.

5 CONCLUSIONS

To conclude, muscle weakness is a comorbidity in patients with a chronic inflammatory disease as rheumatoid arthritis. Muscle weakness can reduce the ability to work and the quality of life for the afflicted persons. Muscle weakness cannot solely be attributed to a decrease in muscle mass. Instead muscle weakness in mice with arthritis and patients with RA is related to intrinsic muscle dysfunction that can be caused by oxPTMs on muscle proteins that are essential for force production, such as actin and RyR1. Stable oxPTMs 3NT and MDA on specific amino acid residues of actin and RyR1 respectively decrease myofibrillar force and impair actin polymerization and increase the open probability of RyR1. The primary sources and scavengers of ROS in pathological conditions as RA need to be further elucidated. Nevertheless, treatment of mice with arthritis with a SOD/catalase mimetic counteracts arthritis-induced muscle weakness. Furthermore, we included patients that were prescribed DMARDs and presented a low rheumatic disease activity, yet they exhibited oxidative stress and muscle weakness. This implies that muscle weakness is a comorbidity that cannot be counteracted by DMARDs (and glucocorticoids) alone and suggests that supplementary pharmacological treatment targeted to improve intrinsic muscle function is needed. There is currently a serious deficit in available clinical therapeutic approaches to counteract muscle weakness. However, the data presented here provide new leads for the development of such targeted treatments, i.e. EUK-134 is an interesting molecular scaffold for future therapeutic interventions to improve muscle function in RA patients. Altogether, the results of this thesis contribute to ultimately improving the quality of life for patients that suffer from muscle weakness caused by a chronic inflammatory disease such as rheumatoid arthritis.

6 ACKNOWLEDGEMENTS

It has now been 11 years ago since I started to study Biomedicine at the Catholic University of Leuven. The journey took me via the University of Lund, where I obtained my Master of Science degree in Biomedicine, to Karolinska Institutet in Stockholm for my PhD. On my path I met many special people who have contributed to where I am now. Hereby I would like to express my sincere gratitude to those persons who made it possible I could get here where I am today.

First, I would like to start by thanking my principle supervisor, Johanna Lanner. You invited me to Stockholm for an interview and gave me a quick tour through the lab and introduced me to your nearest colleagues in the spring of 2014. We started working together on September the 1st that same year also together with Thomas Chaillou. I think us three formed one of the first building stones of the lab group you are leading now. You immediately introduced me to many persons which gave me the opportunity to independently and critically think about which priorities I needed to set in order to successfully start my PhD. Not only then but also after, you have always provided me with knowledge, support and a positive mind-set. I remember sitting with you in the car, driving to the hospital in Huddinge for a meeting with Thomas Gustafsson. I felt my PhD project was going slow and I doubted if I was good enough to ever successfully finish it. You encouraged me that every PhD start is challenging, and that good science takes time. I have always felt that you truly believed in me, my potential and my capabilities from the first day I wrote you an email till the end of my PhD. It is for all these reasons that I am and will forever be thankful that you gave me the opportunity to do my PhD together with you.

Secondly, I would like to thank my current nearest colleagues and friends Theresa, Liu and Baptiste. You guys have not only been amazing the latest weeks, trying to read through all of this thesis and helping me with great input, you have also been supporting me from the day I met you! Working together with you has been great, with good discussions, scientific input and many fun moments (remember that time we tried to rob a bank?). Liu, going with you to Switzerland for the Gordon conference gave me the opportunity to get to know you better. I enjoyed your company on that conference and I hope you liked the cheese fondue. Maja sure remembers that one too. Theresa, thank you for all your help throughout my PhD and of course for all your delicious cakes. Baptiste, you joined the lab only some months ago, however you have already been of great support by wanting to read through all my thesis before submitting it to the printer.

That brings me to all others who have worked in the lab group of Johanna Lanner. Thank you, Thomas Chaillou, Mikaeljohn Kalakoutis, Anna-Lena Boller, Monika Petkovic and above all Niklas Ivarsson. Niklas, you are not able to read this because you are no longer amongst us. Instead of thanking you Niklas, I am writing this to all of you who still are here with us. I learned a lot from Niklas, from force measurements to that hiding bitcoins on a hard drive which you then loose, while bitcoins were worth more than 100.000 Krones a piece, is not such a smart idea. Niklas has supported me from day 1 and I talked with him a lot about all sorts of different things. I am sure you all did as well, and I think the best way to

let somebody live on, is to teach and tell other persons the thing you learned from him, so they can teach and tell that to the generations thereafter.

Not only Thomas, Mikaeljohn, Anna-Lena, Monika and Niklas were giving me scientific support and a great time at Karolinska Institutet, I would also like to thank all my colleagues at the department of Physiology and Pharmacology in Solna for your help and scientific input. Special thanks go also to, Håkan Westerblad, Daniel Andersson, Joseph Burton, Eduardo Uribe Gonzalez, Maja Schlittler, Arthur Cheng, Victoria Wyckelsma and Ellinor Kenne for the close collaboration and scientific input at the department of physiology and pharmacology here at KI. Maja, thank you for the fun at the cheese fondue evening (ps. loved the curtains at Biomedicum). In addition, I would like to thank my colleagues from Jorge Ruas' group for their scientific support: Margareta, Duarte, Shamim, Paula, Paulo, Jorge, Yildiz, Igor, Serge, Michele and Kyle. Last, specially also thanking Divya for helping me with the figures of this thesis!

In addition, I would also like to express my special thanks to my co-supervisors Thomas Gustafsson and Camilla Svensson. Thomas, thank you for all the opportunities you gave me to perform research in the hospital which provided me with "the faces" behind our research: the rheumatoid arthritis patients. That is an experience which truly gave me the motivation to perform biomedical research: to ultimately improve the quality of life for patients that suffer from muscle weakness. Thank you, Camilla, for some good discussions and your knowledge with regards to rheumatoid arthritis. Thereby I would also especially like to thank Katalin Sandor and Kristina Ängeby Möller of the group of Camilla Svensson, for teaching me a lot about the different arthritis models.

My PhD thesis and the great papers we have published would never have been possible without the persons who I collaborated with. Therefore, I would like to thank Malin Persson and Dilson Rassier for all the work you have done and showing me Montreal and McGill University. It was such a good poutine we ate, let's do that again! Thank you Bejan for teaching me how to perform actin polymerization measurements and for your great photoshop skills. I would also especially like to thank Eric Rullman, Karl Olsson, Mats Lilja and Tommy Lundberg at the Karolinska University hospital in Huddinge for your fantastic help with the RA patient study. Thank you also to Roger Karlsson, Nicole Beard, and Ran Friedman and the "Linneaus crew" for your outstanding scientific knowledge and support.

Doing a PhD needs a long-term vision, I once read. I think that doing a PhD needs short term goals besides your PhD. With a sane mind in a sane body we started a field-hockey club. With we, I mean Nils Dreßler and I. We not only started a hockey club, we started a lifestyle with many fantastic moments and goals that we achieved in only 5 years! Becoming Swedish field-hockey champions and the biggest field-hockey club in Sweden have given me joy, fun and knowledge on how to turn ideas to results. The things I learned from you Nils, and all others that contributed to the club, have also helped me in successfully motivating and inspiring people that contributed to my PhD. Therefore, I would like to express my sincere gratitude to all the crew members who are also my great friends: Nils Dreßler, Charlotte

Zwart, Felicity Holmes, Lonneke van Es, Amie Mackenzie, Bas van Zijl, Frank Geldof, Ariadne Schenk, Wouter van der Bijl, Simon Eckerström Liedholm, Flore Kunst, Lars Borm, Rudolf Hermann and Sharon Green. Charlotte Zwart, I would like to especially thank you for always being there for me.

Although I had a long-term vision and short-term goals, my Stockholm adventure and thereby my PhD would never have been fun without my close friends Bas, Boudewijn, Brechtje, Claudia, Emma, Florentine, Gina, Jenny, Jon, Juliette, Thomas and Tosca. Waarde leden, lieve vrienden, het was me een genoegen, lange leven het STHMS Borrelgenootschap! Op naar de volgende borrel zou ik zo zeggen.

Sebastiaan, you have been there for me the last two years. You have not only offered me your place in Amsterdam but also a place in your heart. I will forever be thankful for that and you made me able to finish my PhD.

I would like to end my acknowledgements with thanking my family who have always been there for me and supported me throughout my time abroad: Lieke (and Flip you too), Reinier sr., Carmen, Iwein, Roos, José and Alejandro.

They once told me that the first and the last persons on a paper are the most important ones. Therefore, the last persons I am thanking are my father *Maarten Steinz*, my mother *Marion Steinz* and my brother *Reinier Steinz*. I will choose to thank them in Dutch:

Het is nu 7 jaar geleden dat ik naar Zweden ben verhuisd. Ik heb me vaak afgevraagd waarom ik dat allemaal doe en waarom ik niet dichter bij jullie ben. Ook al kan je elkaar zien via een videoverbinding, echt met elkaar zijn we maar weinig. Vooral als het niet goed gaat met een van ons voel ik me ver van jullie vandaan en zou ik willen dat ik dichterbij was. Jullie hebben echter altijd in mij geloofd, me gesteund en het beste met me voor gehad: "als jij gelukkig bent, dan zijn wij ook gelukkig". Ik ben gelukkig en nu is tijd om naar huis te gaan en alles wat ik van de tijd in het buitenland en van jullie heb geleerd te combineren in een nieuwe start in Nederland. Ik hou van jullie en ik hoop dat jullie nog jaren gezond en gelukkig blijven samen met mij. Dank jullie wel!

7 REFERENCES

1. van Vilsteren M, Boot CR, Knol DL, van Schaardenburg D, Voskuyl AE, Steenbeek R, et al. Productivity at work and quality of life in patients with rheumatoid arthritis. BMC musculoskeletal disorders. 2015;16:107.
2. Yamada T, Fedotovskaya O, Cheng AJ, Cornachione AS, Minozzo FC, Aulin C, et al. Nitrosative modifications of the Ca2+ release complex and actin underlie arthritis-induced muscle weakness. Annals of the rheumatic diseases. 2015;74(10):1907-14.
3. Yamada T, Abe M, Lee J, Tatebayashi D, Himori K, Kanzaki K, et al. Muscle dysfunction associated with adjuvant-induced arthritis is prevented by antioxidant treatment. Skeletal muscle. 2015;5:20.
4. Fraser A, Vallow J, Preston A, Cooper RG. Predicting 'normal' grip strength for rheumatoid arthritis patients. Rheumatology. 1999;38(6):521-8.
5. Hakkinen A, Sokka T, Kotaniemi A, Paananen ML, Malkia E, Kautiainen H, et al. Muscle strength characteristics and central bone mineral density in women with recent onset rheumatoid arthritis compared with healthy controls. Scandinavian journal of rheumatology. 1999;28(3):145-51.
6. C Ekdahl, Broman G. Muscle strength, endurance, and aerobic capacity in rheumatoid arthritis: a comparative study with healthy subjects. Annals of the rheumatic diseases. 1992;51(1):35-40.
7. Waning DL, Mohammad KS, Reiken S, Xie W, Andersson DC, John S, et al. Excess TGF-beta mediates muscle weakness associated with bone metastases in mice. Nature medicine. 2015;21(11):1262-71.
8. Callahan LA, Supinski GS. Sepsis-induced myopathy. Critical care medicine. 2009;37(10 Suppl):S354-67.
9. Rolland Y, Van Kan GA, Gillette-Guyonnet S, Vellas B. Cachexia versus sarcopenia. Current Opinion in Clinical Nutrition and Metabolic Care. 2011;14(1):15-21.
10. Summers GD, Metsios GS, Stavropoulos-Kalinoglou A, Kitas GD. Rheumatoid cachexia and cardiovascular disease. Nature reviews Rheumatology. 2010;6(8):445-51.
11. Walsmith J, Roubenoff R. Cachexia in Rheumatoid Arthritis. Int J Cardiol. 2002;85(1):88-99.
12. Helliwell PS, Jackson S. Relationship between weakness and muscle wasting in rheumatoid arthritis. Annals of the rheumatic diseases. 1994;53(11):726-8.
13. Alamanos Y, Voulgari PV, Drosos AA. Incidence and prevalence of rheumatoid arthritis, based on the 1987 American College of Rheumatology criteria: a systematic review. Seminars in arthritis and rheumatism. 2006;36(3):182-8.
14. Silman AJ, Pearson JE. Epidemiology and genetics of rheumatoid arthritis. Arthritis Res. 2002;4 Suppl 3:S265-72.
15. Smolen JS, Aletaha D, Barton A, Burmester GR, Emery P, Firestein GS, et al. Rheumatoid arthritis. Nature reviews Disease primers. 2018;4:18001.
16. Zhou H, Hu B, Zhaopeng Z, Liu J, Zhong Q, Fan Y, et al. Elevated circulating T cell subsets and cytokines expression in patients with rheumatoid arthritis. Clinical rheumatology. 2019;38(7):1831-9.
17. Deane KD, O'Donnell CI, Hueber W, Majka DS, Lazar AA, Derber LA, et al. The number of elevated cytokines and chemokines in preclinical seropositive rheumatoid arthritis predicts time to diagnosis in an age-dependent manner. Arthritis and rheumatism. 2010;62(11):3161-72.

18. Huffman KM, Jessee R, Andonian B, Davis BN, Narowski R, Huebner JL, et al. Molecular alterations in skeletal muscle in rheumatoid arthritis are related to disease activity, physical inactivity, and disability. Arthritis research & therapy. 2017;19(1):12.
19. Yamada T, Steinz MM, Kenne E, Lanner JT. Muscle Weakness in Rheumatoid Arthritis: The Role of Ca(2+) and Free Radical Signaling. EBioMedicine. 2017;23:12-9.
20. de Palma L, Chillemi C, Albanelli S, Rapali S, Bertoni-Freddari C. Muscle involvement in rheumatoid arthritis: an ultrastructural study. Ultrastructural pathology. 2000;24(3):151-6.
21. Lemmey AB, Wilkinson TJ, Clayton RJ, Sheikh F, Whale J, Jones HS, et al. Tight control of disease activity fails to improve body composition or physical function in rheumatoid arthritis patients. Rheumatology. 2016;55(10):1736-45.
22. Janssen I, Heymsfield SB, Wang ZM, Ross R. Skeletal muscle mass and distribution in 468 men and women aged 18-88 yr. Journal of applied physiology. 2000;89(1):81-8.
23. Frontera WR, Ochala J. Skeletal muscle: a brief review of structure and function. Calcified tissue international. 2015;96(3):183-95.
24. Mukund K, Subramaniam S. Skeletal muscle: A review of molecular structure and function, in health and disease. Wiley Interdiscip Rev Syst Biol Med. 2020;12(1):e1462.
25. Gordon AM, Homsher E, Regnier M. Regulation of contraction in striated muscle. Physiological reviews. 2000;80(2):853-924.
26. Dominguez R, Holmes KC. Actin structure and function. Annual review of biophysics. 2011;40:169-86.
27. Calderon JC, Bolanos P, Caputo C. The excitation-contraction coupling mechanism in skeletal muscle. Biophysical reviews. 2014;6(1):133-60.
28. Sandow A. Excitation-contraction coupling in muscular response. The Yale journal of biology and medicine. 1952;25(3):176-201.
29. Lanner JT, Georgiou DK, Joshi AD, Hamilton SL. Ryanodine receptors: structure, expression, molecular details, and function in calcium release. Cold Spring Harbor perspectives in biology. 2010;2(11):a003996.
30. Spudich JA. The myosin swinging cross-bridge model. Nature reviews Molecular cell biology. 2001;2(5):387-92.
31. Westerblad H, Allen DG. Mechanisms underlying changes of tetanic [Ca2+]i and force in skeletal muscle. Acta Physiol Scand. 1996;156(3):407-16.
32. Chen L, Nelson DR, Zhao Y, Cui Z, Johnston JA. Relationship between muscle mass and muscle strength, and the impact of comorbidities: a population-based, cross-sectional study of older adults in the United States. BMC Geriatr. 2013;13:74.
33. Londhe P, Guttridge DC. Inflammation induced loss of skeletal muscle. Bone. 2015;80:131-42.
34. Tesi C, Colomo F, Piroddi N, Poggesi C. Characterization of the cross-bridge force-generating step using inorganic phosphate and BDM in myofibrils from rabbit skeletal muscles. The Journal of physiology. 2002;541(Pt 1):187-99.
35. Persson M, Steinz MM, Westerblad H, Lanner JT, Rassier DE. Force generated by myosin cross-bridges is reduced in myofibrils exposed to ROS/RNS. American journal of physiology Cell physiology. 2019.
36. Nathan C, Cunningham-Bussel A. Beyond oxidative stress: an immunologist's guide to reactive oxygen species. Nature reviews Immunology. 2013;13(5):349-61.
37. Powers SK, Ji LL, Kavazis AN, Jackson MJ. Reactive oxygen species: impact on skeletal muscle. Compr Physiol. 2011;1(2):941-69.
38. Gronwall C, Amara K, Hardt U, Krishnamurthy A, Steen J, Engstrom M, et al. Autoreactivity to malondialdehyde-modifications in rheumatoid arthritis is linked to disease activity and synovial pathogenesis. Journal of autoimmunity. 2017;84:29-45.

39. Liao CC, Chang YS, Cheng CW, Chi WM, Tsai KL, Chen WJ, et al. Isotypes of autoantibodies against differentially expressed novel malondialdehyde-modified peptide adducts in serum of Taiwanese women with rheumatoid arthritis. Journal of proteomics. 2018;170:141-50.
40. Khojah HM, Ahmed S, Abdel-Rahman MS, Hamza AB. Reactive oxygen and nitrogen species in patients with rheumatoid arthritis as potential biomarkers for disease activity and the role of antioxidants. Free radical biology & medicine. 2016;97:285-91.
41. Lillig CH, Berndt C. Glutaredoxins in thiol/disulfide exchange. Antioxidants & redox signaling. 2013;18(13):1654-65.
42. Ayala A, Munoz MF, Arguelles S. Lipid peroxidation: production, metabolism, and signaling mechanisms of malondialdehyde and 4-hydroxy-2-nonenal. Oxidative medicine and cellular longevity. 2014;2014:360438.
43. Radi R. Protein tyrosine nitration: biochemical mechanisms and structural basis of functional effects. Accounts of chemical research. 2013;46(2):550-9.
44. Radi R, Beckman JS, Bush KM, Freeman BA. Peroxynitrite-induced membrane lipid peroxidation: the cytotoxic potential of superoxide and nitric oxide. Archives of biochemistry and biophysics. 1991;288(2):481-7.
45. Lanner JT, Georgiou DK, Dagnino-Acosta A, Ainbinder A, Cheng Q, Joshi AD, et al. AICAR prevents heat-induced sudden death in RyR1 mutant mice independent of AMPK activation. Nature medicine. 2012;18(2):244-51.
46. Hohn A, Konig J, Grune T. Protein oxidation in aging and the removal of oxidized proteins. Journal of proteomics. 2013;92:132-59.
47. Ohshima H, Friesen M, Brouet I, Bartsch H. Nitrotyrosine as a new marker for endogenous nitrosation and nitration of proteins. Food and chemical toxicology : an international journal published for the British Industrial Biological Research Association. 1990;28(9):647-52.
48. Beckman JS, Beckman TW, Chen J, Marshall PA, Freeman BA. Apparent hydroxyl radical production by peroxynitrite: implications for endothelial injury from nitric oxide and superoxide. Proceedings of the National Academy of Sciences of the United States of America. 1990;87(4):1620-4.
49. Botti H, Moller MN, Steinmann D, Nauser T, Koppenol WH, Denicola A, et al. Distance-dependent diffusion-controlled reaction of *NO and O2*- at chemical equilibrium with ONOO. The journal of physical chemistry B. 2010;114(49):16584-93.
50. Souza JM, Peluffo G, Radi R. Protein tyrosine nitration--functional alteration or just a biomarker? Free radical biology & medicine. 2008;45(4):357-66.
51. Fedorova M, Kuleva N, Hoffmann R. Reversible and irreversible modifications of skeletal muscle proteins in a rat model of acute oxidative stress. Biochimica et biophysica acta. 2009;1792(12):1185-93.
52. Zhao J, Chen J, Zhu H, Xiong YL. Mass spectrometric evidence of malonaldehyde and 4-hydroxynonenal adductions to radical-scavenging soy peptides. Journal of agricultural and food chemistry. 2012;60(38):9727-36.
53. Mateen S, Moin S, Khan AQ, Zafar A, Fatima N. Increased Reactive Oxygen Species Formation and Oxidative Stress in Rheumatoid Arthritis. PloS one. 2016;11(4):e0152925.
54. Andrade FH, Reid MB, Allen DG, Westerblad H. Effect of hydrogen peroxide and dithiothreitol on contractile function of single skeletal muscle fibres from the mouse. The Journal of physiology. 1998;509 (Pt 2):565-75.
55. Dutka TL, Mollica JP, Lamb GD. Differential effects of peroxynitrite on contractile protein properties in fast- and slow-twitch skeletal muscle fibers of rat. Journal of applied physiology. 2011;110(3):705-16.
56. Martin-Romero FJ, Gutiérrez-Martin Y, Hanao F, Gutiérrez-Merino C. Fluorescence measurements of steady state peroxynitrite production upon SIN-1

decomposition: NADH versus dihydrodichlorofluorescein and dihydrorhodamine 123. J Fluoresc. 2004;14(1):17-23.
57. Supinski G, Stofan D, Callahan LA, Nethery D, Nosek TM, DiMarco A. Peroxynitrite induces contractile dysfunction and lipid peroxidation in the diaphragm. Journal of applied physiology. 1999;87(2):783-91.
58. Canton M, Neverova I, Menabo R, Van Eyk J, Di Lisa F. Evidence of myofibrillar protein oxidation induced by postischemic reperfusion in isolated rat hearts. American journal of physiology Heart and circulatory physiology. 2004;286(3):H870-7.
59. Bowen TS, Mangner N, Werner S, Glaser S, Kullnick Y, Schrepper A, et al. Diaphragm muscle weakness in mice is early-onset post-myocardial infarction and associated with elevated protein oxidation. Journal of applied physiology. 2015;118(1):11-9.
60. Aksenov MY, Aksenova MV, Butterfield DA, Geddes JW, Markesbery WR. Protein oxidation in the brain in Alzheimer's disease. Neuroscience. 2001;103(2):373-83.
61. Pastore A, Tozzi G, Gaeta LM, Bertini E, Serafini V, Di Cesare S, et al. Actin glutathionylation increases in fibroblasts of patients with Friedreich's ataxia: a potential role in the pathogenesis of the disease. The Journal of biological chemistry. 2003;278(43):42588-95.
62. Lu J, Katano T, Uta D, Furue H, Ito S. Rapid S-nitrosylation of actin by NO-generating donors and in inflammatory pain model mice. Mol Pain. 2011;7:101.
63. Holmes KC, Popp D, Gebhard WK, W. Atomic Model of the actin filament. Nature 1990;347:44-9.
64. Graceffa P, Dominguez R. Crystal structure of monomeric actin in the ATP state. Structural basis of nucleotide-dependent actin dynamics. The Journal of biological chemistry. 2003;278(36):34172-80.
65. Oda T, Iwasa M, Aihara T, Maeda Y, Narita A. The nature of the globular- to fibrous-actin transition. Nature. 2009;457(7228):441-5.
66. Schuler H. ATPase activity and conformational changes in the regulation of actin. Biochimica et biophysica acta. 2001;1549(2):137-47.
67. Lehrer SS, Geeves MA. The muscle thin filament as a classical cooperative/allosteric regulatory system. Journal of molecular biology. 1998;277(5):1081-9.
68. Merino F, Pospich S, Funk J, Wagner T, Kullmer F, Arndt HD, et al. Structural transitions of F-actin upon ATP hydrolysis at near-atomic resolution revealed by cryo-EM. Nat Struct Mol Biol. 2018;25(6):528-37.
69. Galkin VE, Orlova A, Schroder GF, Egelman EH. Structural polymorphism in F-actin. Nat Struct Mol Biol. 2010;17(11):1318-23.
70. Fujii T, Namba K. Structure of actomyosin rigour complex at 5.2 A resolution and insights into the ATPase cycle mechanism. Nat Commun. 2017;8:13969.
71. Allen DG, Westerblad H. The effects of caffeine on intracellular calcium, force and the rate of relaxation of mouse skeletal muscle. The Journal of physiology. 1995;487 (Pt 2):331-42.
72. Lanner JT. Ryanodine receptor physiology and its role in disease. Advances in experimental medicine and biology. 2012;740:217-34.
73. Yuchi Z, Van Petegem F. Ryanodine receptors under the magnifying lens: Insights and limitations of cryo-electron microscopy and X-ray crystallography studies. Cell calcium. 2016;59(5):209-27.
74. des Georges A, Clarke OB, Zalk R, Yuan Q, Condon KJ, Grassucci RA, et al. Structural Basis for Gating and Activation of RyR1. Cell. 2016;167(1):145-57 e17.
75. Santulli G, Lewis D, des Georges A, Marks AR, Frank J. Ryanodine Receptor Structure and Function in Health and Disease. Sub-cellular biochemistry. 2018;87:329-52.
76. Zalk R, Clarke OB, des Georges A, Grassucci RA, Reiken S, Mancia F, et al. Structure of a mammalian ryanodine receptor. Nature. 2015;517(7532):44-9.

77. Yuchi Z, Yuen SM, Lau K, Underhill AQ, Cornea RL, Fessenden JD, et al. Crystal structures of ryanodine receptor SPRY1 and tandem-repeat domains reveal a critical FKBP12 binding determinant. Nat Commun. 2015;6:7947.
78. Yan Z, Bai X, Yan C, Wu J, Li Z, Xie T, et al. Structure of the rabbit ryanodine receptor RyR1 at near-atomic resolution. Nature. 2015;517(7532):50-5.
79. Meissner G. Regulation of Ryanodine Receptor Ion Channels Through Posttranslational Modifications. Current topics in membranes. 2010;66:91-113.
80. Andersson DC, Betzenhauser MJ, Reiken S, Meli AC, Umanskaya A, Xie W, et al. Ryanodine receptor oxidation causes intracellular calcium leak and muscle weakness in aging. Cell metabolism. 2011;14(2):196-207.
81. Takeshima H, Nishimura S, Matsumoto T, Ishida H, Kangawa K, Minamino N, et al. Primary structure and expression from complementary DNA of skeletal muscle ryanodine receptor. Nature. 1989;339(6224):439-45.
82. Zorzato F, Fujii J, Otsu K, Phillips M, Green NM, Lai FA, et al. Molecular cloning of cDNA encoding human and rabbit forms of the Ca2+ release channel (ryanodine receptor) of skeletal muscle sarcoplasmic reticulum. The Journal of biological chemistry. 1990;265(4):2244-56.
83. Andronache Z, Hamilton SL, Dirksen RT, Melzer W. A retrograde signal from RyR1 alters DHP receptor inactivation and limits window Ca2+ release in muscle fibers of Y522S RyR1 knock-in mice. Proceedings of the National Academy of Sciences of the United States of America. 2009;106(11):4531-6.
84. Santulli G, Nakashima R, Yuan Q, Marks AR. Intracellular calcium release channels: an update. The Journal of physiology. 2017;595(10):3041-51.
85. Bellinger AM, Reiken S, Carlson C, Mongillo M, Liu X, Rothman L, et al. Hypernitrosylated ryanodine receptor calcium release channels are leaky in dystrophic muscle. Nature medicine. 2009;15(3):325-30.
86. Moore CP, Rodney G, Zhang JZ, Santacruz-Toloza L, Strasburg G, Hamilton SL. Apocalmodulin and Ca2+ calmodulin bind to the same region on the skeletal muscle Ca2+ release channel. Biochemistry. 1999;38(26):8532-7.
87. Chaube R, Hess DT, Wang YJ, Plummer B, Sun QA, Laurita K, et al. Regulation of the skeletal muscle ryanodine receptor/Ca2+-release channel RyR1 by S-palmitoylation. The Journal of biological chemistry. 2014;289(12):8612-9.
88. Sun J, Xu L, Eu JP, Stamler JS, Meissner G. Nitric oxide, NOC-12, and S-nitrosoglutathione modulate the skeletal muscle calcium release channel/ryanodine receptor by different mechanisms. An allosteric function for O2 in S-nitrosylation of the channel. The Journal of biological chemistry. 2003;278(10):8184-9.
89. Sun J, Xin C, Eu JP, Stamler JS, Meissner G. Cysteine-3635 is responsible for skeletal muscle ryanodine receptor modulation by NO. Proceedings of the National Academy of Sciences of the United States of America. 2001;98(20):11158-62.
90. Stange M, Xu L, Balshaw D, Yamaguchi N, Meissner G. Characterization of recombinant skeletal muscle (Ser-2843) and cardiac muscle (Ser-2809) ryanodine receptor phosphorylation mutants. The Journal of biological chemistry. 2003;278(51):51693-702.
91. Jacko D, Bersiner K, Friederichs G, Ritter P, Nirenberg L, Eisenbraun J, et al. Resistance exercise-induced muscle fatigue is not accompanied by increased phosphorylation of ryanodine receptor 1 at serine 2843. PloS one. 2018;13(6):e0199307.
92. Reiken S, Lacampagne A, Zhou H, Kherani A, Lehnart SE, Ward C, et al. PKA phosphorylation activates the calcium release channel (ryanodine receptor) in skeletal muscle: defective regulation in heart failure. The Journal of cell biology. 2003;160(6):919-28.
93. Rullman E, Andersson DC, Melin M, Reiken S, Mancini DM, Marks AR, et al. Modifications of skeletal muscle ryanodine receptor type 1 and exercise intolerance in heart

failure. The Journal of heart and lung transplantation : the official publication of the International Society for Heart Transplantation. 2013;32(9):925-9.
94. Hood DA, Memme JM, Oliveira AN, Triolo M. Maintenance of Skeletal Muscle Mitochondria in Health, Exercise, and Aging. Annu Rev Physiol. 2019;81:19-41.
95. Zhao RZ, Jiang S, Zhang L, Yu ZB. Mitochondrial electron transport chain, ROS generation and uncoupling (Review). Int J Mol Med. 2019;44(1):3-15.
96. Murphy MP. How mitochondria produce reactive oxygen species. Biochem J. 2009;417(1):1-13.
97. Cheng AJ, Yamada T, Rassier DE, Andersson DC, Westerblad H, Lanner JT. Reactive oxygen/nitrogen species and contractile function in skeletal muscle during fatigue and recovery. The Journal of physiology. 2016;594(18):5149-60.
98. Cadenas E, Boveris A, Ragan CI, Stoppani AO. Production of superoxide radicals and hydrogen peroxide by NADH-ubiquinone reductase and ubiquinol-cytochrome c reductase from beef-heart mitochondria. Archives of biochemistry and biophysics. 1977;180(2):248-57.
99. Platzer A, Nussbaumer T, Karonitsch T, Smolen JS, Aletaha D. Analysis of gene expression in rheumatoid arthritis and related conditions offers insights into sex-bias, gene biotypes and co-expression patterns. PloS one. 2019;14(7):e0219698.
100. Panga V, Kallor AA, Nair A, Harshan S, Raghunathan S. Mitochondrial dysfunction in rheumatoid arthritis: A comprehensive analysis by integrating gene expression, protein-protein interactions and gene ontology data. PloS one. 2019;14(11):e0224632.
101. Panday A, Sahoo MK, Osorio D, Batra S. NADPH oxidases: an overview from structure to innate immunity-associated pathologies. Cellular & molecular immunology. 2015;12(1):5-23.
102. Sakellariou GK, Jackson MJ, Vasilaki A. Redefining the major contributors to superoxide production in contracting skeletal muscle. The role of NAD(P)H oxidases. Free radical research. 2014;48(1):12-29.
103. Luo S, Lei H, Qin H, Xia Y. Molecular mechanisms of endothelial NO synthase uncoupling. Curr Pharm Des. 2014;20(22):3548-53.
104. Stuehr D, Pou S, Rosen GM. Oxygen reduction by nitric-oxide synthases. The Journal of biological chemistry. 2001;276(18):14533-6.
105. Nethery D, Callahan LA, Stofan D, Mattera R, DiMarco A, Supinski G. PLA(2) dependence of diaphragm mitochondrial formation of reactive oxygen species. Journal of applied physiology. 2000;89(1):72-80.
106. Zuo L, Christofi FL, Wright VP, Bao S, Clanton TL. Lipoxygenase-dependent superoxide release in skeletal muscle. Journal of applied physiology. 2004;97(2):661-8.
107. Kozakowska M, Pietraszek-Gremplewicz K, Jozkowicz A, Dulak J. The role of oxidative stress in skeletal muscle injury and regeneration: focus on antioxidant enzymes. J Muscle Res Cell Motil. 2015;36(6):377-93.
108. Culotta VC, Yang M, O'Halloran TV. Activation of superoxide dismutases: putting the metal to the pedal. Biochimica et biophysica acta. 2006;1763(7):747-58.
109. Sepasi Tehrani H, Moosavi-Movahedi AA. Catalase and its mysteries. Prog Biophys Mol Biol. 2018;140:5-12.
110. Pascual-Ahuir A, Manzanares-Estreder S, Proft M. Pro- and Antioxidant Functions of the Peroxisome-Mitochondria Connection and Its Impact on Aging and Disease. Oxidative medicine and cellular longevity. 2017;2017:9860841.
111. Fransen M, Lismont C, Walton P. The Peroxisome-Mitochondria Connection: How and Why? Int J Mol Sci. 2017;18(6).
112. Singh H, Arya S, Talapatra P, Lather K, Mathur R, Singhania A, et al. Assessment of fatigue in rheumatoid arthritis (by Functional Assessment of Chronic Illness

Therapy-Fatigue score) and its relation to disease activity and anemia. J Clin Rheumatol. 2014;20(2):87-90.
113. Smolen JS, Landewe R, Bijlsma J, Burmester G, Chatzidionysiou K, Dougados M, et al. EULAR recommendations for the management of rheumatoid arthritis with synthetic and biological disease-modifying antirheumatic drugs: 2016 update. Annals of the rheumatic diseases. 2017;76(6):960-77.
114. Smolen JS, Steiner G. Therapeutic strategies for rheumatoid arthritis. Nature reviews Drug discovery. 2003;2(6):473-88.
115. Cheng AJ, Westerblad H. Mechanical isolation, and measurement of force and myoplasmic free [Ca(2+)] in fully intact single skeletal muscle fibers. Nature protocols. 2017;12(9):1763-76.
116. Cornachione AS, Leite F, Bagni MA, Rassier DE. The increase in non-cross-bridge forces after stretch of activated striated muscle is related to titin isoforms. American journal of physiology Cell physiology. 2016;310(1):C19-26.
117. Leite FS, Minozzo FC, Kalganov A, Cornachione AS, Cheng YS, Leu NA, et al. Reduced passive force in skeletal muscles lacking protein arginylation. American journal of physiology Cell physiology. 2016;310(2):C127-35.
118. Shalabi N, Cornachione A, de Souza Leite F, Vengallatore S, Rassier DE. Residual force enhancement is regulated by titin in skeletal and cardiac myofibrils. The Journal of physiology. 2017;595(6):2085-98.
119. Choi L, Liu Z, Matthews CE, Buchowski MS. Validation of accelerometer wear and nonwear time classification algorithm. Medicine and science in sports and exercise. 2011;43(2):357-64.
120. Freedson PS, Melanson E, Sirard J. Calibration of the Computer Science and Applications, Inc. accelerometer. Medicine and science in sports and exercise. 1998;30(5):777-81.
121. Kouyama T, Mihashi K. Fluorimetry study of N-(1-pyrenyl)iodoacetamide-labelled F-actin. Local structural change of actin protomer both on polymerization and on binding of heavy meromyosin. Eur J Biochem. 1981;114(1):33-8.
122. Houk TW, Jr., Ue K. The measurement of actin concentration in solution: a comparison of methods. Anal Biochem. 1974;62(1):66-74.
123. Nesvizhskii AI, Keller A, Kolker E, Aebersold R. A statistical model for identifying proteins by tandem mass spectrometry. Analytical chemistry. 2003;75(17):4646-58.
124. Larkin MA, Blackshields G, Brown NP, Chenna R, McGettigan PA, McWilliam H, et al. Clustal W and Clustal X version 2.0. Bioinformatics. 2007;23(21):2947-8.
125. Van Der Spoel D, Lindahl E, Hess B, Groenhof G, Mark AE, Berendsen HJ. GROMACS: fast, flexible, and free. Journal of computational chemistry. 2005;26(16):1701-18.
126. Lorenz M, Holmes KC. The actin-myosin interface. Proceedings of the National Academy of Sciences of the United States of America. 2010;107(28):12529-34.
127. Saunders MG, Voth GA. Water molecules in the nucleotide binding cleft of actin: effects on subunit conformation and implications for ATP hydrolysis. Journal of molecular biology. 2011;413(1):279-91.
128. Baker JL, Voth GA. Effects of ATP and actin-filament binding on the dynamics of the myosin II S1 domain. Biophysical journal. 2013;105(7):1624-34.
129. Best RB, Zhu X, Shim J, Lopes PE, Mittal J, Feig M, et al. Optimization of the additive CHARMM all-atom protein force field targeting improved sampling of the backbone phi, psi and side-chain chi(1) and chi(2) dihedral angles. J Chem Theory Comput. 2012;8(9):3257-73.

130. Hess B, Bekker H, Berendsen HJC, Fraaije JGEM. LINCS: A linear constraint solver for molecular simulations. Journal of computational chemistry. 1997;18(12):1463-72.
131. Parrinello M, Rahman A. Polymorphic Transitions in Single-Crystals - a New Molecular-Dynamics Method. J Appl Phys. 1981;52(12):7182-90.
132. Ewald PP. Die Berechnung optischer und elektrostatischer Gitterpotentiale. Annalen der Physik. 1921;369(3):253-87.
133. Darden T, York D, Pedersen L. Particle Mesh Ewald - an N.Log(N) Method for Ewald Sums in Large Systems. J Chem Phys. 1993;98(12):10089-92.
134. Hanson GT, Aggeler R, Oglesbee D, Cannon M, Capaldi RA, Tsien RY, et al. Investigating mitochondrial redox potential with redox-sensitive green fluorescent protein indicators. The Journal of biological chemistry. 2004;279(13):13044-53.
135. Pal R, Basu Thakur P, Li S, Minard C, Rodney GG. Real-time imaging of NADPH oxidase activity in living cells using a novel fluorescent protein reporter. PloS one. 2013;8(5):e63989.
136. Verhoeven F, Tordi N, Prati C, Demougeot C, Mougin F, Wendling D. Physical activity in patients with rheumatoid arthritis. Joint Bone Spine. 2016;83(3):265-70.
137. Neuberger GB, Aaronson LS, Gajewski B, Embretson SE, Cagle PE, Loudon JK, et al. Predictors of exercise and effects of exercise on symptoms, function, aerobic fitness, and disease outcomes of rheumatoid arthritis. Arthritis and rheumatism. 2007;57(6):943-52.
138. Mahdy MAA. Skeletal muscle fibrosis: an overview. Cell Tissue Res. 2019;375(3):575-88.
139. Khairallah RJ, Shi G, Sbrana F, Prosser BL, Borroto C, Mazaitis MJ, et al. Microtubules underlie dysfunction in duchenne muscular dystrophy. Science signaling. 2012;5(236):ra56.
140. Bellinger AM, Reiken S, Carlson C, Mongillo M, Liu X, Rothman L, et al. Hypernitrosylated ryanodine receptor calcium release channels are leaky in dystrophic muscle. Nat Med. 2009;15(3):325-30.
141. Eliasson MJ, Huang Z, Ferrante RJ, Sasamata M, Molliver ME, Snyder SH, et al. Neuronal nitric oxide synthase activation and peroxynitrite formation in ischemic stroke linked to neural damage. The Journal of neuroscience : the official journal of the Society for Neuroscience. 1999;19(14):5910-8.
142. Mihm MJ, Yu F, Carnes CA, Reiser PJ, McCarthy PM, Van Wagoner DR, et al. Impaired myofibrillar energetics and oxidative injury during human atrial fibrillation. Circulation. 2001;104(2):174-80.
143. Hussain SN, Cornachione AS, Guichon C, Al Khunaizi A, Leite Fde S, Petrof BJ, et al. Prolonged controlled mechanical ventilation in humans triggers myofibrillar contractile dysfunction and myofilament protein loss in the diaphragm. Thorax. 2016;71(5):436-45.
144. Picard M, Jung B, Liang F, Azuelos I, Hussain S, Goldberg P, et al. Mitochondrial dysfunction and lipid accumulation in the human diaphragm during mechanical ventilation. American journal of respiratory and critical care medicine. 2012;186(11):1140-9.
145. Stehle R, Kruger M, Pfitzer G. Force kinetics and individual sarcomere dynamics in cardiac myofibrils after rapid ca(2+) changes. Biophysical journal. 2002;83(4):2152-61.
146. Stehle R, Kruger M, Scherer P, Brixius K, Schwinger RH, Pfitzer G. Isometric force kinetics upon rapid activation and relaxation of mouse, guinea pig and human heart muscle studied on the subcellular myofibrillar level. Basic research in cardiology. 2002;97 Suppl 1:I127-35.
147. Telley IA, Stehle R, Ranatunga KW, Pfitzer G, Stussi E, Denoth J. Dynamic behaviour of half-sarcomeres during and after stretch in activated rabbit psoas myofibrils:

sarcomere asymmetry but no 'sarcomere popping'. The Journal of physiology. 2006;573(Pt 1):173-85.
148. Clements MK, Siemsen DW, Swain SD, Hanson AJ, Nelson-Overton LK, Rohn TT, et al. Inhibition of actin polymerization by peroxynitrite modulates neutrophil functional responses. Journal of leukocyte biology. 2003;73(3):344-55.
149. Fujii T, Iwane AH, Yanagida T, Namba K. Direct visualization of secondary structures of F-actin by electron cryomicroscopy. Nature. 2010;467(7316):724-8.
150. Aslan M, Ryan TM, Townes TM, Coward L, Kirk MC, Barnes S, et al. Nitric oxide-dependent generation of reactive species in sickle cell disease. Actin tyrosine induces defective cytoskeletal polymerization. The Journal of biological chemistry. 2003;278(6):4194-204.
151. Baek K, Liu X, Ferron F, Shu S, Korn ED, Dominguez R. Modulation of actin structure and function by phosphorylation of Tyr-53 and profilin binding. Proceedings of the National Academy of Sciences of the United States of America. 2008;105(33):11748-53.
152. Liu X, Shu S, Hong MS, Levine RL, Korn ED. Phosphorylation of actin Tyr-53 inhibits filament nucleation and elongation and destabilizes filaments. Proceedings of the National Academy of Sciences of the United States of America. 2006;103(37):13694-9.
153. Liu X, Shu S, Hong MS, Yu B, Korn ED. Mutation of actin Tyr-53 alters the conformations of the DNase I-binding loop and the nucleotide-binding cleft. The Journal of biological chemistry. 2010;285(13):9729-39.
154. Bayden AS, Yakovlev VA, Graves PR, Mikkelsen RB, Kellogg GE. Factors influencing protein tyrosine nitration--structure-based predictive models. Free radical biology & medicine. 2011;50(6):749-62.
155. Souza JM, Daikhin E, Yudkoff M, Raman CS, Ischiropoulos H. Factors determining the selectivity of protein tyrosine nitration. Archives of biochemistry and biophysics. 1999;371(2):169-78.
156. Ishii T, Ito S, Kumazawa S, Sakurai T, Yamaguchi S, Mori T, et al. Site-specific modification of positively-charged surfaces on human serum albumin by malondialdehyde. Biochemical and biophysical research communications. 2008;371(1):28-32.
157. Heijnen HF, van Donselaar E, Slot JW, Fries DM, Blachard-Fillion B, Hodara R, et al. Subcellular localization of tyrosine-nitrated proteins is dictated by reactive oxygen species generating enzymes and by proximity to nitric oxide synthase. Free radical biology & medicine. 2006;40(11):1903-13.
158. Place N, Ivarsson N, Venckunas T, Neyroud D, Brazaitis M, Cheng AJ, et al. Ryanodine receptor fragmentation and sarcoplasmic reticulum Ca2+ leak after one session of high-intensity interval exercise. Proceedings of the National Academy of Sciences of the United States of America. 2015;112(50):15492-7.
159. Cheng AJ, Bruton JD, Lanner JT, Westerblad H. Antioxidant treatments do not improve force recovery after fatiguing stimulation of mouse skeletal muscle fibres. The Journal of physiology. 2015;593(2):457-72.
160. Durham WJ, Aracena-Parks P, Long C, Rossi AE, Goonasekera SA, Boncompagni S, et al. RyR1 S-nitrosylation underlies environmental heat stroke and sudden death in Y522S RyR1 knockin mice. Cell. 2008;133(1):53-65.
161. Rodney GG, Williams BY, Strasburg GM, Beckingham K, Hamilton SL. Regulation of RYR1 activity by Ca(2+) and calmodulin. Biochemistry. 2000;39(26):7807-12.
162. Meissner G, Darling E, Eveleth J. Kinetics of rapid Ca2+ release by sarcoplasmic reticulum. Effects of Ca2+, Mg2+, and adenine nucleotides. Biochemistry. 1986;25(1):236-44.
163. Kimlicka L, Lau K, Tung CC, Van Petegem F. Disease mutations in the ryanodine receptor N-terminal region couple to a mobile intersubunit interface. Nat Commun. 2013;4:1506.

164. Yamazawa T, Takeshima H, Shimuta M, Iino M. A region of the ryanodine receptor critical for excitation-contraction coupling in skeletal muscle. The Journal of biological chemistry. 1997;272(13):8161-4.
165. Lau K, Chan MM, Van Petegem F. Lobe-specific calmodulin binding to different ryanodine receptor isoforms. Biochemistry. 2014;53(5):932-46.
166. Ahern GP, Junankar PR, Dulhunty AF. Ryanodine receptors from rabbit skeletal muscle are reversibly activated by rapamycin. Neurosci Lett. 1997;225(2):81-4.
167. Matecki S, Dridi H, Jung B, Saint N, Reiken SR, Scheuermann V, et al. Leaky ryanodine receptors contribute to diaphragmatic weakness during mechanical ventilation. Proceedings of the National Academy of Sciences of the United States of America. 2016;113(32):9069-74.
168. Marx SO, Reiken S, Hisamatsu Y, Jayaraman T, Burkhoff D, Rosemblit N, et al. PKA phosphorylation dissociates FKBP12.6 from the calcium release channel (ryanodine receptor): defective regulation in failing hearts. Cell. 2000;101(4):365-76.
169. Henderson CA, Gomez CG, Novak SM, Mi-Mi L, Gregorio CC. Overview of the Muscle Cytoskeleton. Compr Physiol. 2017;7(3):891-944.
170. Rambourg A, Segretain D. Three-dimensional electron microscopy of mitochondria and endoplasmic reticulum in the red muscle fiber of the rat diaphragm. Anat Rec. 1980;197(1):33-48.
171. Picard M, White K, Turnbull DM. Mitochondrial morphology, topology, and membrane interactions in skeletal muscle: a quantitative three-dimensional electron microscopy study. Journal of applied physiology. 2013;114(2):161-71.
172. Meyer AJ, Dick TP. Fluorescent protein-based redox probes. Antioxidants & redox signaling. 2010;13(5):621-50.
173. Lukyanov KA, Belousov VV. Genetically encoded fluorescent redox sensors. Biochimica et biophysica acta. 2014;1840(2):745-56.
174. Cadenas E, Davies KJ. Mitochondrial free radical generation, oxidative stress, and aging. Free radical biology & medicine. 2000;29(3-4):222-30.
175. Turrens JF. Mitochondrial formation of reactive oxygen species. The Journal of physiology. 2003;552(Pt 2):335-44.
176. Hidalgo C, Sanchez G, Barrientos G, Aracena-Parks P. A transverse tubule NADPH oxidase activity stimulates calcium release from isolated triads via ryanodine receptor type 1 S -glutathionylation. The Journal of biological chemistry. 2006;281(36):26473-82.
177. Ferreira LF, Laitano O. Regulation of NADPH oxidases in skeletal muscle. Free radical biology & medicine. 2016;98:18-28.
178. Himori K, Abe M, Tatebayashi D, Lee J, Westerblad H, Lanner JT, et al. Superoxide dismutase/catalase mimetic EUK-134 prevents diaphragm muscle weakness in monocrotalin-induced pulmonary hypertension. PloS one. 2017;12(2):e0169146.